iScience

CellPress
OPEN ACCESS

Article

Identification of new ETV6 modulators through a high-throughput functional screening

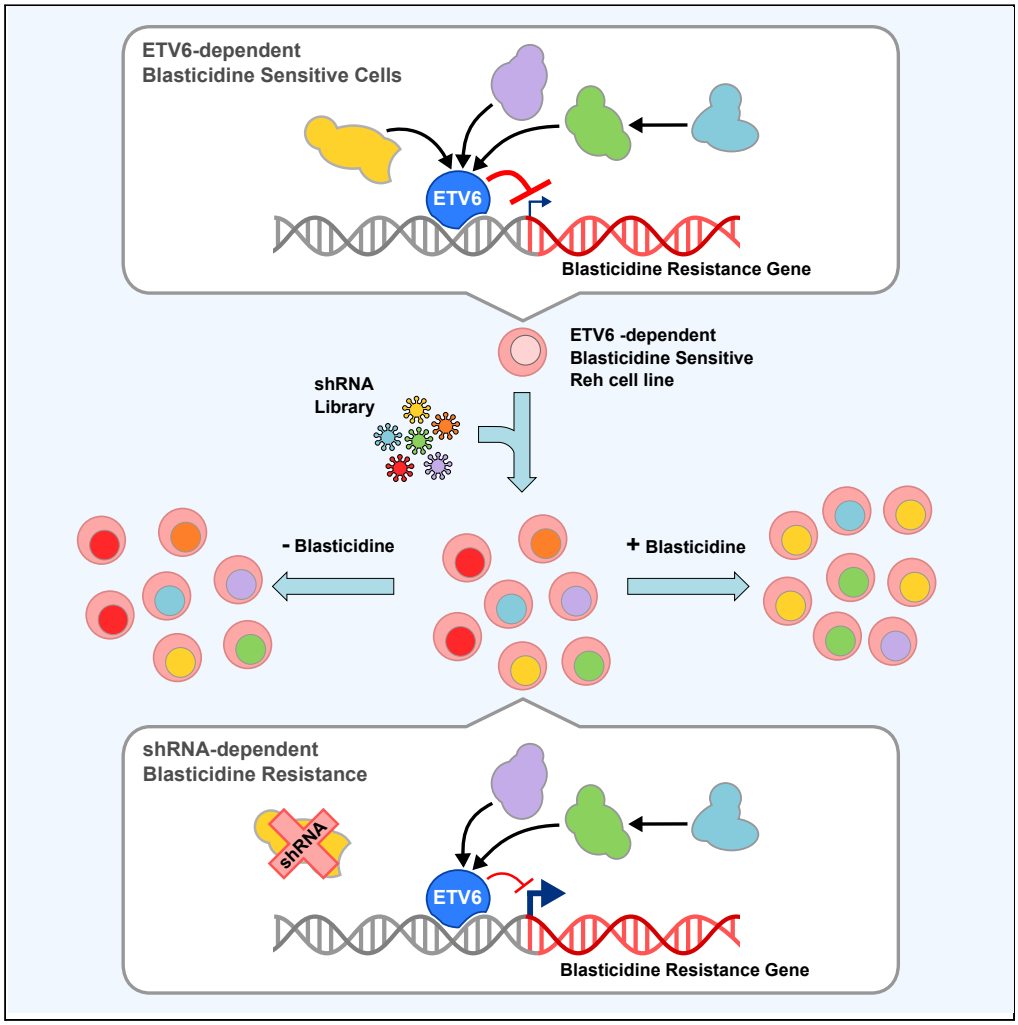

Benjamin Neveu, Chantal Richer, Pauline Cassart, ..., Nicolas Garnier, Stéphane Gobeil, Daniel Sinnett

daniel.sinnett@umontreal.ca (D.S.)
stephane.gobeil@crchudequebec.ulaval.ca (S.G.)

Highlights

We develop a genome-wide shRNAs screen for ETV6 modulators

The screen uncovered 13 novel putative ETV6 modulator genes

The modulators demonstrated a broad impact on the *ETV6* transcriptional network

T-ALL cells results suggest modulators are conserved in other cellular contexts

Neveu et al., iScience *25*, 103858
March 18, 2022
https://doi.org/10.1016/j.isci.2022.103858

iScience

CellPress
OPEN ACCESS

Article

Identification of new ETV6 modulators through a high-throughput functional screening

Benjamin Neveu,[1,2] Chantal Richer,[1] Pauline Cassart,[1] Maxime Caron,[1,3] Camille Jimenez-Cortes,[1,4] Pascal St-Onge,[1] Claire Fuchs,[1,2] Nicolas Garnier,[1] Stéphane Gobeil,[5,6,*] and Daniel Sinnett[1,7,8,*]

SUMMARY

***ETV6* transcriptional activity is critical for proper blood cell development in the bone marrow. Despite the accumulating body of evidence linking *ETV6* malfunction to hematological malignancies, its regulatory network remains unclear. To uncover genes that modulate *ETV6* repressive transcriptional activity, we performed a specifically designed, unbiased genome-wide shRNA screen in pre-B acute lymphoblastic leukemia cells. Following an extensive validation process, we identified 13 shRNAs inducing overexpression of *ETV6* transcriptional target genes. We showed that the silencing of *AKIRIN1*, *COMMD9*, *DYRK4*, *JUNB*, and *SRP72* led to an abrogation of *ETV6* repressive activity. We identified critical modulators of the *ETV6* function which could participate in cellular transformation through the *ETV6* transcriptional network.**

INTRODUCTION

ETV6 is a member of the ETS (E26 transformation-specific) superfamily of transcription factors (Mavrothalassitis and Ghysdael, 2000) located on the short arm of chromosome 12. ETS transcription factors have been associated with multiple biological processes and pathways with, among others, critical implications in hematopoiesis (Ciau-Uitz et al., 2013). Their dysregulation correlates with hematological diseases such as lymphomas, leukemia, and myelodysplastic syndrome. Chromosomal abnormalities of the 12p13 band are frequently found in these malignancies. So far, more than 30 fusion partners have been identified in *ETV6*-derived translocations (De Braekeleer et al., 2012). The mechanisms through which these fusions induce transformation are highly variable and depend on the function of the partner as well as the retained domains of *ETV6*. In some cases, the expected impact of the translocation is to inhibit *ETV6* normal function as proposed for the translocations t(1; 12)(q21; p13) (Otsubo et al., 2010) and t(12; 21)(p13; q22) (Romana et al., 1995a; Golub et al., 1995; Gunji et al., 2004).

The t(12; 21)(p13; q22) translocation is one of the most frequent chromosomal abnormalities found in childhood B-cell acute lymphoblastic leukemia (ALL) and is characteristic of the ETV6-RUNX1 ALL subtype (Romana et al., 1995b; Shurtleff et al., 1995; Bhojwani et al., 2015). It fuses all functional domains encoded by the *AML1* (*RUNX1*) gene to the first five exons of *ETV6* encoding its Pointed (PD) and repression domains. Despite the high recurrence of t(12; 21) in B-cell ALL and the resulting expression of the ETV6-AML1 fusion protein in patients with t(12; 21) positive leukemic (Agape et al., 1997; Poirel et al., 1998), the t(12; 21) was shown to be insufficient to induce leukemic transformation (Andreasson et al., 2001; van der Weyden et al., 2011; Mori et al., 2002). Interestingly, the non-rearranged residual allele of *ETV6* is targeted by deleterious events in most cases of t(12; 21) positive ALL (Poirel et al., 1998; Patel et al., 2003; Lilljebjorn et al., 2010; Montpetit et al., 2004), suggesting that *ETV6* inactivation could play a critical role in leukemogenesis. In addition, several groups recently reported germline mutations in *ETV6* that were associated with familial hematological disorders (Moriyama et al., 2015; Topka et al., 2015; Noetzli et al., 2015; Zhang et al., 2015). Several of these mutations were in the ETS DNA-binding domain of *ETV6* and impaired its nuclear localization and/or repressor activity. These findings strongly support a role for *ETV6*-mediated transcription in these malignancies.

Despite the consequences of *ETV6* dysfunction, very little is known about its regulatory network. To negatively regulate transcription, *ETV6* cooperates with co-repressors such as the N-CoR and mSin3A complexes and the histone deacetylase *HDAC3* (Lee et al., 2004; Wang and Hiebert, 2001; Guidez et al.,

[1]Sainte-Justine University Health Center Research Center, Montreal, QC H3T 1C5, Canada

[2]Department of Biochemistry and Molecular Medicine, Faculty of Medicine, University of Montreal, Montreal, QC H3C 3J7, Canada

[3]Department of Human Genetics, McGill University, Montréal, QC H3A 0C7, Canada

[4]Molecular Biology Program, Faculty of Medicine, University of Montreal, Montreal, QC H3C 3J7, Canada

[5]CHU de Québec-Université Laval Research Center, Quebec City, QC G1V 4G2, Canada

[6]Department of Molecular Medicine, Faculty of Medicine, Université Laval, Quebec City, QC G1V 0A6, Canada

[7]Department of Pediatrics, Faculty of Medicine, University of Montreal, Montreal, QC H3C 3J7, Canada

[8]Lead contact

*Correspondence: daniel.sinnett@umontreal.ca (D.S.), stephane.gobeil@crchudequebec.ulaval.ca (S.G.)

https://doi.org/10.1016/j.isci.2022.103858

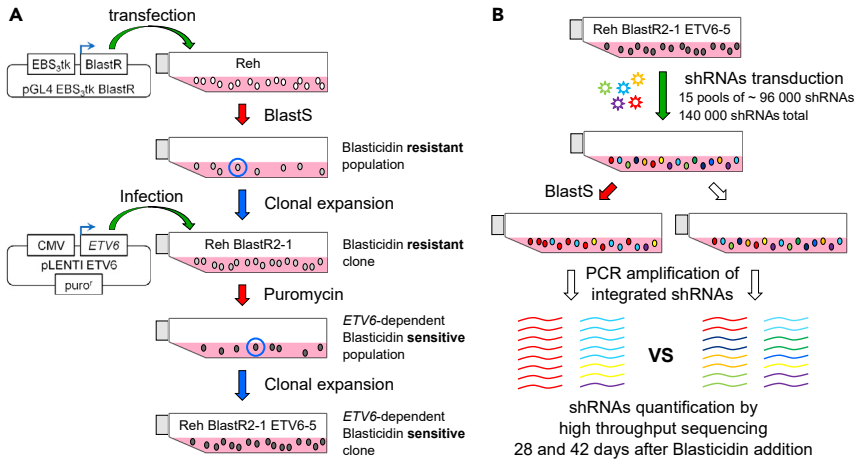

Figure 1. Overview of the genome-wide shRNA screening design

(A) To identify putative modulators of *ETV6*-mediated transcriptional repression, a pre-B acute lymphoblastic leukemia cell line (Reh) was modified sequentially to obtain an *ETV6*-dependent Blasticidin sensitive clone. These cells are expressing the Blasticidin-resistance gene (BlastR) under the control of the *ETV6*-responsive artificial promoter (EBS_3tk). (B) These cells were then transduced with shRNAs ($n \approx 140{,}000$) and selected with Blasticidin. Over-represented shRNAs in the Blasticidin condition compared to the mock condition are expected to target genes required for *ETV6*-mediated repression of BlastR.

2000). *ETV6* interaction with *HDAC3* was shown to be modulated through its binding with the *IRF-8* transcription factor (Kuwata et al., 2002). This interaction was further associated with a change in *ETV6* binding and transcriptional activity. Although indicating that *ETV6*-mediated transcription can be regulated through complex interactions, these studies were conducted by candidate gene or interaction-based approaches and did not investigate the full intricacy of *ETV6* function.

Small hairpin RNAs (shRNAs) are widely used to silence gene expression (Azlan et al., 2016). In this study, we designed a cellular screening strategy to functionally interrogate the impact of over 140,000 shRNAs on *ETV6*-mediated gene repression. A panel of high priority genes selected from the screen results were further examined for their capacity to efficiently regulate *ETV6* activity by monitoring its transcriptional network in pre-B ALL cells (Neveu et al., 2016, 2018). Validation experiments unveiled key modulators of *ETV6* repressive function in leukemic cells.

RESULTS

Generating *ETV6*-dependent Blasticidin sensitive cells

To gain insights into the network of *ETV6* modulators, we modified the Reh pre-B ALL cell line (Figure 1A) to develop a genome-wide shRNAs screen for ETV6 modulators (Figure 1B). A Blasticidin-resistance gene (BlastR) was stably integrated and expressed through an artificial *ETV6*-responsive promoter (EBS_3tk) composed of three tandem ETV6 binding sites (EBS) (Szymczyna and Arrowsmith, 2000) followed by the HSV-TK promoter. Reh cells were selected because they lack endogenous *ETV6* expression as a result of a t(12; 21)(p13; q22) translocation and the 12p13 deletion of the non-translocated allele (Uphoff et al., 1997). In absence of functional endogenous *ETV6*, EBS_3tk is active and promotes Blasticidin resistance in this modified cell line. Wild-type *ETV6* was then re-introduced through lentiviral transduction in isolated blasticidin resistant clones. Ectopically expressed *ETV6* is expected to bind and repress the EBS_3tk promoter leading to reduce BlastR expression. As shown in Figure 2A, BlastR expression in the Reh EBS_3tk BlastR clone2-1 is significantly reduced upon *ETV6* expression compared to the mock and pLENTI control clones (2.7-fold compared to pLENTI; p value ≤ 0.001). We derived a final clone from the Reh EBS_3tk BlastR clone2-1 expressing ETV6 to obtain a robust and homogeneous cellular system which we refer to as clone 2-1 ETV6-5.

Although each Reh EBS_3tk BlastR clone significantly expressed *ETV6* after transduction (Figure 2A, inset), the inconsistent effect on BlastR repression suggests that the chromatin context where EBS_3tk BlastR inserted is rather influential. To identify the integration site of EBS_3tk BlastR in the ETV6-responsive clone 2-1, we used data from a previous *ETV6* chromatin immunoprecipitation sequencing experiment (ChIP-seq)

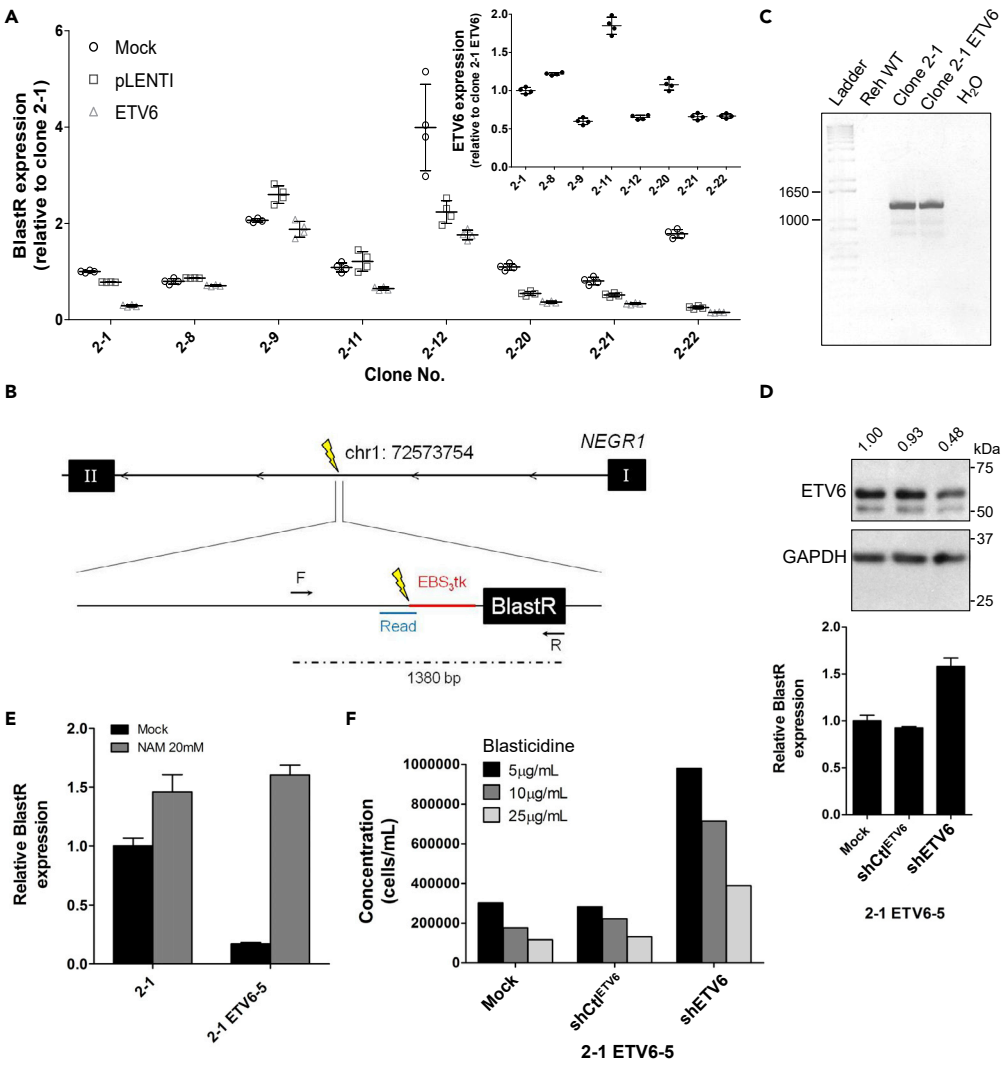

Figure 2. Establishment of an *ETV6*-dependent Blasticidin-sensitive leukemia cell system

(A) BlastR expression was evaluated by qRT-PCR in each Reh EBS$_3$tk BlastR clone (clones 2-1 to 2-22) following *ETV6* expression (inset). Data points for technical replicates are shown with lines indicating mean ± SD (n = 4).

(B) *ETV6* ChIP-seq data obtained from clone 2-1 located the insertion site of EBS$_3$tk BlastR (yellow mark). One sequencing read (indicated in blue) contained the partial sequence of EBS3tk promoter together with 95 nucleotides of the first intron of the *NEGR1* gene. The F/R arrows depict the primers used in the PCR analysis. The dash line represent the amplified fragment (1380 bp) generated by PCR.

(C) PCR analysis of the clone 2-1 confirmed the insertion site of EBS$_3$tk BlastR in the first intron of the *NEGR1* gene.

(D) BlastR expression was evaluated by qRT-PCR in 2-1 ETV6-5 cells after shRNA-mediated silencing of *ETV6* (quantified Western blot) or (E) after nicotinamide (NAM) treatment. Data are shown as mean ± SD, n = 4.

(F) 2-1 ETV6-5, shCtl$^{ETV6-GFP}$, and shETV6-GFP sorted cells were maintained in culture for 12 days with various Blasticidin concentrations and counted to evaluate proliferation.

performed with clone 2-1 (Neveu et al., 2018). Several reads mapped on the EBS$_3$tk promoter, suggesting that *ETV6* is effectively recruited to the artificial promoter. One read contained the partial sequence of the EBS$_3$tk promoter merged with a sequence from the first intron of the *NEGR1* gene, indicating the integration site (Figure 2B). PCR analysis of the Reh EBS$_3$tk BlastR clone 2-1 confirmed the integration site of EBS$_3$tk BlastR in the intron one of *NEGR1* (Figure 2C). Based on previous transcriptome data (Neveu et al., 2016), this integration did not impact *NEGR1* expression compared to non-modified Reh cells (53.1 and 51.3 FPKM, respectively). Furthermore, *NEGR1* is not significantly modulated by *ETV6* re-expression (logFoldChange = −0.46, FDR = 0.50). Together, these results indicate that EBS$_3$tk BlastR insertion at an active locus

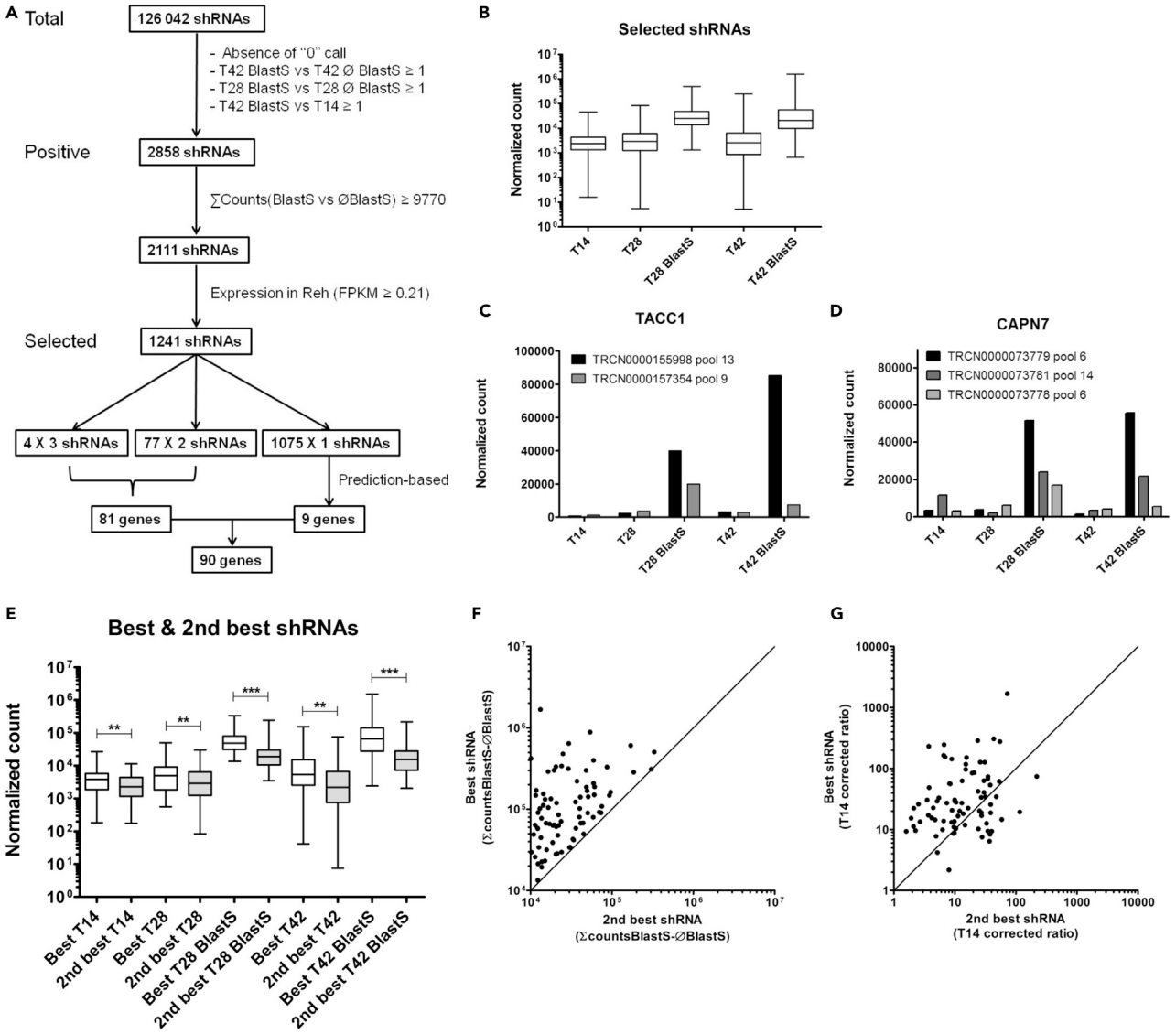

Figure 3. Genome-wide shRNA screening to identify *ETV6* modulators

(A) Flowchart illustrating the stepwise procedure for the analysis of the genome-wide shRNA screen sequencing.

(B) Normalized read counts distribution of the 1241 selected shRNAs shown for the five time points. Whiskers represent minimum and maximum.

(C–D). Examples of selected shRNAs normalized counts for the five time points.

(E) Normalized count distributions are shown separately for the best and second-best shRNAs of a pair or trio. Whiskers represent minimum and maximum; statistical significance is calculated with a paired Student *t* test (n = 81) (***p < 0.001, **p < 0.01).

(F) Relation between the best (*y* axis) and second-best (*x* axis) shRNAs of a pair or trio according to their respective Blasticidin count difference.

(G) The same relation between the best (*y* axis) and second-best (*x* axis) shRNAs of a pair or trio when their Blasticidin count difference is divided by their initial count at T_{14}. See also Tables S1 and S2.

enables stable BlastR expression, accessibility to *ETV6*, and concomitant *ETV6*-mediated gene repression through the EBS_3tk promoter.

To validate that *ETV6*-mediated repression of BlastR is reversible, we introduced in the 2-1 ETV6-5 clone an shRNA against *ETV6* (shETV6) or negative control ($shCtl^{ETV6}$) with GFP coexpression. The GFP positive fraction of cells was retrieved and *ETV6* knockdown was confirmed at the protein level (Figure 2D). As expected, BlastR expression was positively modulated by *ETV6* knockdown (Figure 2D). Treatment with, nicotinamide (NAM), which is used as an inhibitor of epigenetic repression (Schmidt et al., 2004; Bitterman et al., 2002; Sanders et al., 2010), increased BlastR expression in the 2-1 ETV6-5 clone (Figure 2E), further

indicating that the repression is reversible. Finally, as expected the BlastR expression observed in shETV6 cells (Figure 2D) considerably increased their proliferation in the presence of Blasticidin (Figure 2F). Altogether, these results demonstrate that the modified Reh cell lines EBS_3tk BlastR 2-1 ETV6-5 clone is a suitable model to screen for modulators of *ETV6* repressive activity.

Identification of putative *ETV6* modulators through a genome-wide shRNA screen

We designed a genome-wide loss-of-function screen to identify *ETV6* modulators (Figure 1B). Cells expressing shRNAs impairing *ETV6* repressive activity are expected to increase BlastR expression and be selectively enriched following a blasticidin treatment. Fourteen days following transduction with the complete Mission lentiviral shRNA library (~140,000 unique shRNAs split into 15 pools), deep sequencing genomic DNA allowed the identification of 126,042 unique integrated shRNAs, which were evenly distributed among the 15 pools. By applying a series of thresholds outlined in Figure 3A and the STAR Methods section, we selected 2,858 positive shRNAs that were over-represented in presence of Blasticidine (BlastS condition) at both the 28 and 42-day time points compared to their respective control population without selection. From those, 1,241 shRNAs were retained (Figure 3B and Table S1) after discarding those with a non-significant over-representation (i.e. $\sum$Counts(BlastS vs ØBlastS) less than 2 SD of the SHC202 control; see STAR Methods section) as well as those targeting unexpressed genes (FPKM $\leq$0.21 (Hart et al., 2013)) in Reh cells (Neveu et al., 2016). As expected, among these selected shRNAs, one shRNA against *ETV6* was enriched in the BlastS conditions. 1,075 genes were targeted by a single shRNA (Figure 3A) and, with few exceptions (see below), were not further considered to avoid potential off-target effects. Nonetheless, 77 and four genes (total of 81 targets) were targeted by two and three distinct shRNAs, respectively, and were thus prioritized (Figure 3A, and Table S2). Interestingly, 33 of these 81 genes were targeted by shRNAs from different pools (for example *TACC1* and *CAPN7*, Figures 3C and 3D, respectively; see also Table S2), suggesting that their selection was not dependent on the other shRNAs present in their respective pool.

The shRNA with the greater difference in normalized counts between Blasticidin and control conditions, for a given pair or trio, was selected for further validation (Figures 3E and 3F). Interestingly, although the differences between the two best shRNAs are mostly attributed to their representations in Blasticidin conditions (T_{28} BlastS and T_{42} BlastS), the best shRNAs are better represented in control conditions (T_{28} and T_{42}) as well as in their initial populations prior to Blasticidin selection (T_{14}) (Figure 3E). To attenuate biases, the difference in normalized counts between Blasticidin and control conditions for each shRNA were divided by their representation at T_{14} (Figure 3G). The relationship between the best and second-best shRNAs is, indeed, less divergent after implementing this correction (compare Figures 3F and 3G), indicating that two shRNAs targeting the same gene are likely to promote a similar impact on Blasticidin resistance. Accordingly, only the shRNAs with the strongest impact were selected (Table S2).

To identify additional candidates among the 1,075 single shRNAs, we used a complementary approach based on structure predictions (Singh et al., 2010). We identified 136 proteins predicted to interact with at least three of the 81 selected ETV6 modulators identified above. Nine of these were part of the group of 1,075 genes targeted by a single shRNAs and were likely valid candidates. They were thus added to the 81 candidates for a total of 90 genes (Figure 3A and Table S2).

Validation of putative *ETV6* modulators on known endogenous transcriptional targets

To validate the impact of the putative modulators on *ETV6*-mediated regulation, we constructed distinct Reh *ETV6* cell lines expressing an shRNA against each of these candidates and evaluated the *ETV6* transcriptional network (Neveu et al., 2016) by targeted RNA sequencing (refer to STAR Methods) using a custom panel of genes. Of the 84 putative *ETV6* target genes included in the panel, 40 were confirmed as their expression was significantly reduced in Reh in an *ETV6* dependent manner (Figure 4A and Table S3). Of those, 22 are associated with *ETV6* ChIP-seq signal (Neveu et al., 2018) and are considered direct *ETV6* targets. Inversely, the expression of 64 genes previously shown to be independent of *ETV6* (Neveu et al., 2016) behaves similarly in the current targeted RNA-seq experiment (Figure 4B and Table S3). As expected most (62/64) were not associated with *ETV6* ChIP-seq signals (Neveu et al., 2018) and were used as negative controls (Table S3).

We calculated the number of direct *ETV6* targets (n = 22) affected by the shRNA tested, as compared to the negative shRNA controls (SHC002 and SHC202). 24 shRNAs led to a specific overexpression of *ETV6* targets (n = 22) compared to *ETV6*-unrelated genes (n = 62) (Figure 4C), indicating that their effects on gene expression are likely mediated by impairing *ETV6* repressive function.

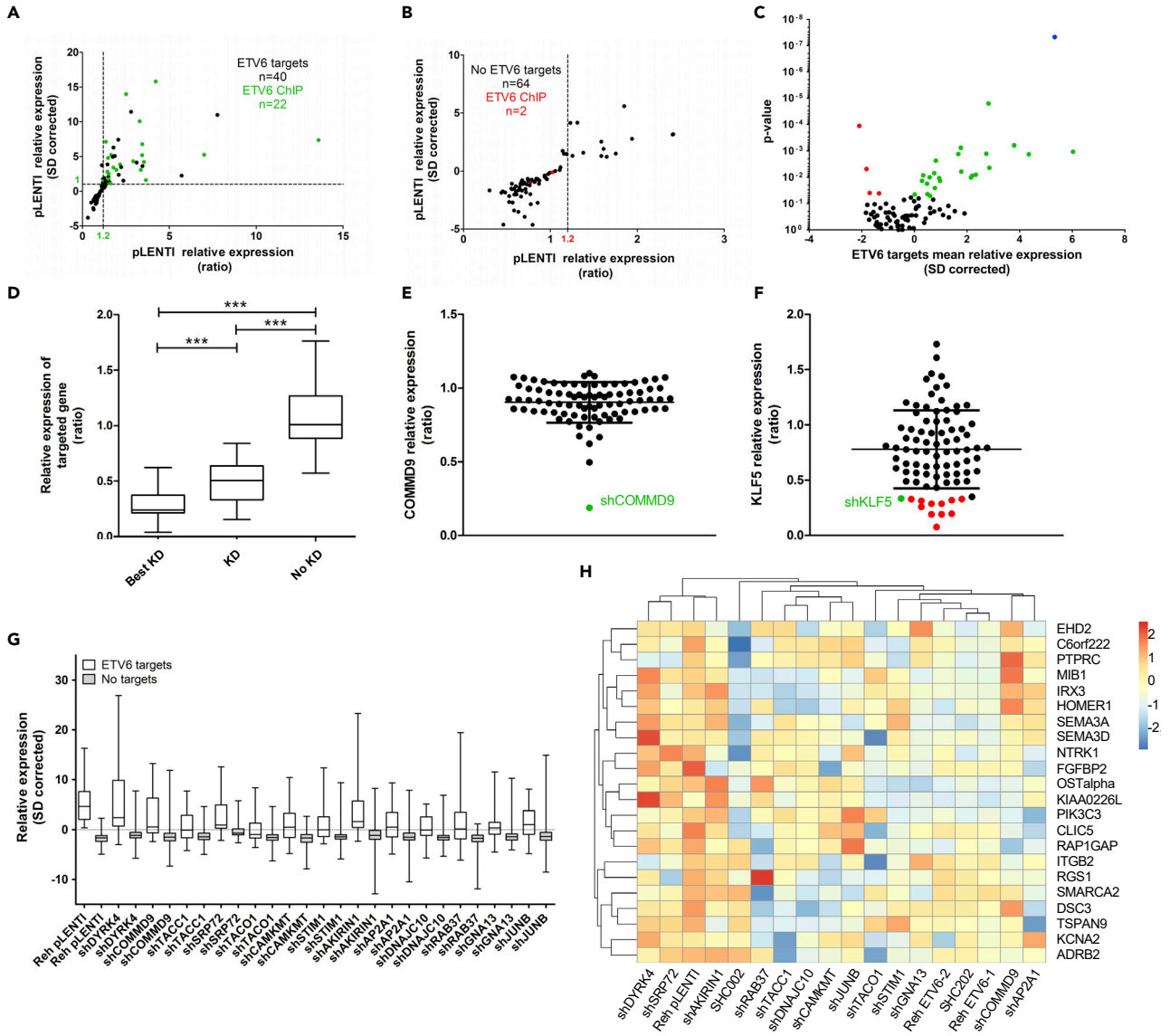

Figure 4. Impact of putative *ETV6* modulators on its transcriptional regulatory network

(A) Graphical representation of the relative expression of *ETV6* target genes or (B) *ETV6*-independent control genes in the pLENTI control sample compared to the *ETV6*-expressing controls.

(C) The mean relative expression of *ETV6* targets (*x* axis) is compared to the relative expression of control genes obtained with the same shRNA; the Student's *t* test p values are shown on the *y* axis. Colored dots (green: overexpressed; red: underexpressed) are significant shRNAs. The blue dot represents the Reh pLENTI sample which lacks *ETV6* expression and serves as a positive control.

(D) Relative expression of the shRNA-targeted genes according to the category of knockdown. Best knockdown (Best KD), n = 31; Knockdown (KD), n = 32; No knockdown (No KD), n = 22). Whiskers represent minimum and maximum; statistical significance is calculated with an unpaired Student's *t* test (***$p < 0.001$).

(E) Relative *COMMD9* expression is shown for all shRNA samples. shCOMMD9 sample is shown in green and displays the lowest expression. Lines represent mean ± SD.

(F) Relative *KLF5* expression is diminished in the shKLF5 sample (green) but several other shRNAs also reduce its expression. Lines represent mean ± SD.

(G) Distribution of the relative expressions of *ETV6* targets (n = 22) and control genes (n = 62) in the 13 significant shRNA samples. Reh pLENTI is also shown as a control. Whiskers represent minimum and maximum.

(H) Heatmap representation of the normalized read counts of *ETV6* targets (lanes) in the 13 significant shRNA samples (and control samples; columns). See also Figure S1 and Table S3.

Analyses of the expression level of shRNAs-targeted genes by RNA sequencing revealed that from the 90 candidate genes, 85 have a detectable expression (informative amplicons). The shRNAs were categorized into three groups based on their silencing patterns (Figure 4D). The ''Best knockdown'' group (n = 31) led to

Table 1. Data summary of the five top *ETV6* modulators

	Gene symbol		AKIRIN1	COMMD9	DYRK4	JUNB	SRP72
	shRNA		TRCN0000134954	TRCN0000167758	TRCN0000197116	TRCN0000014943	TRCN0000151445
Genome-wide shRNA screen	Pool		12	11	13	2	15
	Normalized counts	T14	2822	1196	5864	178	5250
		T28	1563	1538	15,253	1131	14,583
		T28 BlastS	41,303	16,880	56,508	9936	163,516
		T42	1306	1835	14,864	656	17,490
		T42 BlastS	24,629	27,894	37,829	12,352	199,618
	∑BlastS-ØBlastS counts		63,063	41,401	64,221	20,500	331,062
	T14 corrected ratio		22.35	34.61	10.95	115.39	63.06
Targeted sequencing validation	KD efficiency (remaining expression)		38.73%	18.78%	26.84%	19.44%	48.82%
	Number of overexpressed targets (≥1 SD)		15	10	16	11	10
	Mean targets relative expression	SD corrected	4.35	2.73	6.03	1.67	2.85
		Ratio	2.10	1.93	3.21	1.99	2.55
	Mean controls relative expression	SD corrected	−1.07	−1.13	−0.76	−1.04	−0.15
		Ratio	0.78	0.71	0.77	0.76	0.93
	Student's *t* test p value	Targets vs no targets	0.00133	0.00127	0.00106	0.00129	0.00434
		Targets SHC vs shRNA (paired)	0.00669	0.01284	0.00281	0.02227	0.00564

T14, T28, and T42 represent the timepoints (days after transduction), KD, knockdown; SD, standard deviation.

the lowest expression of their target gene (mean silencing of 71%) among all samples (e.g. shCOMMD9, Figure 4E). The shRNAs in the ''Knockdown'' group (n = 32) demonstrate a silencing effect on their target gene but are not the shRNA with the strongest effect on their target (e.g. shKLF5, Figure 4F). Consequently, their effects could not be clearly associated with their target gene. Finally, the ''No knockdown'' group (n = 22) failed to repress its target gene.

From the 31 shRNA in the ''best knockdown'' group, 12 led to significantly overexpressed *ETV6* targets and one was validated by qPCR (*DYRK4*, 73% knockdown) because its RNA targeted sequencing was too low for interpretation (Figure S1). Altogether, we identified 13 shRNAs that efficiently knocked down their target genes and impaired *ETV6* transcriptional activity (Figure 4G). However, the overexpression levels and the number of *ETV6* targets affected by the silencing of these putative modulators are variable, suggesting that they could act in a gene-specific manner (Figures 4G and 4H). To determine the most influential *ETV6* modulators, we compared the expression of *ETV6* targets in each shRNA sample to SHC controls. Among the 13 selected shRNAs, 5 (shAKIRIN1, shCOMMD9, shDYRK4, shJUNB, and shSRP72) significantly impacted the expression of *ETV6* target genes (Table 1). Moreover, an unsupervised clustering analysis based on the expression of the 22 *ETV6* targets revealed the critical influence of *AKIRIN1*, *DYRK4*, and *SRP72* depletion on *ETV6* function as these shRNA samples clustered in a distinct group including Reh pLENTI sample lacking *ETV6* expression (Figure 4H).

ETV6-modulated transcription of t(12; 21)-associated genes

Leukemic cells from patients with t(12; 21) positive have distinct and clear expression profiles (Yeoh et al., 2002). This molecular signature can be, at least partly, explained by the absence of *ETV6* expression as some of its target genes are specifically overexpressed in these cells (Neveu et al., 2016). Interestingly, nine of the 22 *ETV6* target genes included in the validation process were identified as being specifically overexpressed in patients t(12; 21) positive (Neveu et al., 2016).

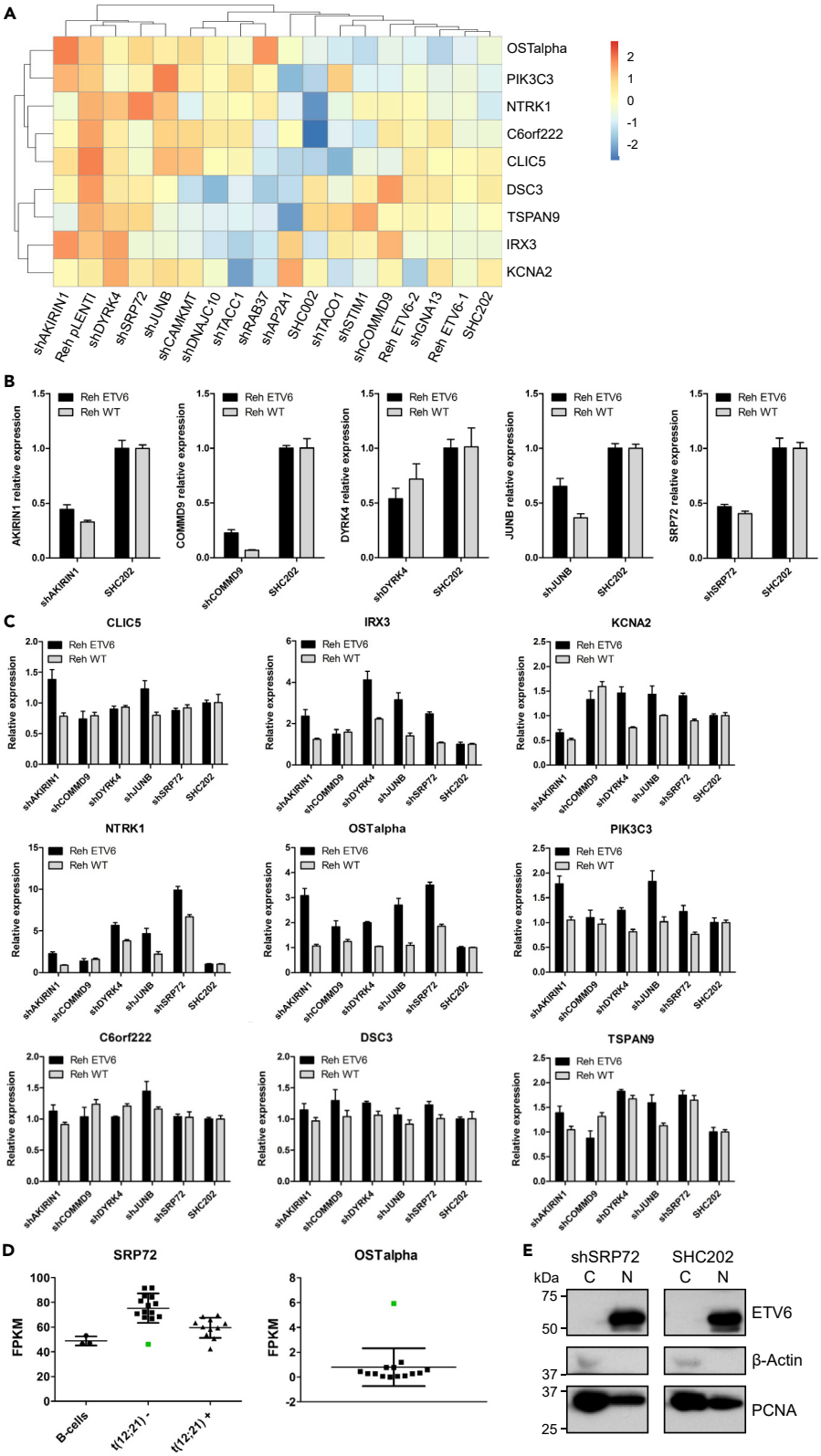
A
OSTalpha
PIK3C3
NTRK1
C6orf222
CLIC5
DSC3
TSPAN9
IRX3
KCNA2
2
1
0
-1
-2
shAKIRIN1
Reh pLENTI
shDYRK4
shSRP72
shJUNB
shCAMKMT
shDNAJC10
shTACC1
shRAB37
shAP2A1
SHC002
shTACO1
shSTIM1
shCOMMD9
Reh ETV6-2
shGNA13
Reh ETV6-1
SHC202
B
Reh ETV6
Reh WT
AKIRIN1 relative expression
COMMD9 relative expression
DYRK4 relative expression
JUNB relative expression
SRP72 relative expression
shAKIRIN1
SHC202
shCOMMD9
shDYRK4
shJUNB
shSRP72
C
CLIC5
IRX3
KCNA2
NTRK1
OSTalpha
PIK3C3
C6orf222
DSC3
TSPAN9
Relative expression
D
SRP72
OSTalpha
FPKM
B-cells
t(12;21) -
t(12;21) +
E
shSRP72
SHC202
kDa
C
N
75
50
37
25
ETV6
β-Actin
PCNA

Figure 5. Impact of the top *ETV6* modulators on the transcription of t(12; 21)-associated overexpressed genes

(A) Heatmap representation of the normalized read counts of the 9 t(12; 21)-associated *ETV6* targets (lanes) in the 13 significant shRNA samples (and control samples; columns).

(B) Relative expression of the five top *ETV6* modulators after shRNAs transduction. Data are shown as mean ± SD, n = 6.

(C) Relative expression of the t(12; 21)-associated *ETV6* target genes in both Reh WT and Reh *ETV6* cells upon silencing of *ETV6* modulators. Data are shown as mean ± SD, n = 6.

(D) *SRP72* (left) and *OSTalpha* (right) expression in leukemic patient samples. The green dot represents the same patient. Lines represent mean ± SD.

(E) Impact of *SRP72* on the *ETV6* protein. *ETV6* expression and localization (C: cytoplasm; N: nucleus) was evaluated by Western blotting in Reh *ETV6* shSRP72 and SHC202 control cells. See also Figures S2 and S3, and Table S4.

Unsupervised clustering analysis with the 9 t(12; 21) associated target genes showed that four of the 13 selected modulators, *AKIRIN1*, *DYRK4*, *SRP72*, and *JUNB* clustered with the pLENTI sample (Figure 5A). Of the five top modulators (Table 1), only *COMMD9* showed a moderate impact on t(12; 21)-associated *ETV6* targets (Figure 5A).

We confirmed that the 9 t(12; 21)-associated *ETV6* targets were downregulated in Reh *ETV6* compared to Reh wild-type (WT) cells (Figure S2). We then silenced each of the top five *ETV6* modulators in both cellular backgrounds (Figure 5B) and further evaluated their impact on gene expression (Figure 5C). The silencing of *AKIRIN1*, *DYRK4*, *JUNB*, and *SRP72* upregulated most of the *ETV6* targets, whereas *COMMD9* knockdown showed less impact (Figure 5C). Of note, *OSTalpha* is the only *ETV6* target to be significatively overexpressed by the silencing of all five modulators. Overexpression of the t(12; 21)-associated *ETV6* target genes was mostly restricted to Reh *ETV6* cells (Figure 5C, Reh *ETV6* vs Reh WT), indicating that the observed upregulations are, indeed, owing to the impairment of *ETV6*-mediated repression.

We next investigated the expression status of the *ETV6* modulators in childhood ALL patients. No clear association could be made between the expression of *AKIRIN1*, *COMMD9*, *DYRK4*, and *JUNB* and t(12; 21)-associated *ETV6* targets (data not shown). However, the expression of *SRP72* was significantly lower (Figure 5D, left) and, the expression of *OSTalpha* strikingly upregulated (Figure 5D, right) in one of the t(12; 21) negative samples. This result strengthens the role of *SRP72* in *ETV6* repressive function in patients with pre-B ALL. However, *ETV6* protein level and localization remain unchanged after *SRP72* silencing (Figure 5E), suggesting that *SRP72* plays a role in *ETV6*-mediated repression through an alternate pathway.

Recently the ALL subtype ETV6-RUNX1-like has been identified (Lilljebjorn et al., 2016). It is characterized by expression profiles similar to the ETV6-RUNX1 subtype in absence of the defining ETV6-RUNX1 t(12; 21) rearrangement. Using a balanced set of patients' RNA-seq data (n = 16) from the Mullighan study (Gu et al., 2019) we investigated the difference in expression between *ETV6* modulators expression in both subtypes (Figure S3). Only DNAJC10 is differentially expressed in the two subtypes (Wilcoxon p value = 0.0011). However, the difference in expression between the two subtypes remains small.

Implications of *ETV6* and its modulators in pre-T acute lymphoblastic leukemia

ETV6 transcriptional function is associated with childhood pre-B ALL (Bhojwani et al., 2015) but remains elusive in other cancers. We thus investigated *ETV6*-mediated transcription in pre-T ALL with particular attention to its newly identified modulators.

We measured the expression of known *ETV6* targets in patients with pre-T ALL (Lajoie et al., 2017). Interestingly, one of them showed significant overexpression of *CLIC5* (Figure 6A, arrow), a known *ETV6* target gene strongly upregulated in patients with t(12; 21) positive pre-B ALL (Figure 6A) (Neveu et al., 2016). Strikingly, an *ETV6* deletion was found in this patient (Spinella et al., 2016), suggesting that *CLIC5* overexpression is attributed to *ETV6* depletion. To test this, we knocked down *ETV6* in the pre-T leukemic cell line MOLT4 and found that *CLIC5* expression, but not that of other t(12; 21)-associated *ETV6* targets, is significantly upregulated (Figure 6B, inset), demonstrating that *CLIC5* gene is an *ETV6* target in pre-T cells. We then evaluated the implication of the five top *ETV6* modulators on *CLIC5* expression. shRNA-mediated silencing was validated for each modulator (Figure S4) and knockdowns were equivalent to those obtained in Reh cells (Figure 5B). Remarkably, repression of all five *ETV6* modulators induced a significant

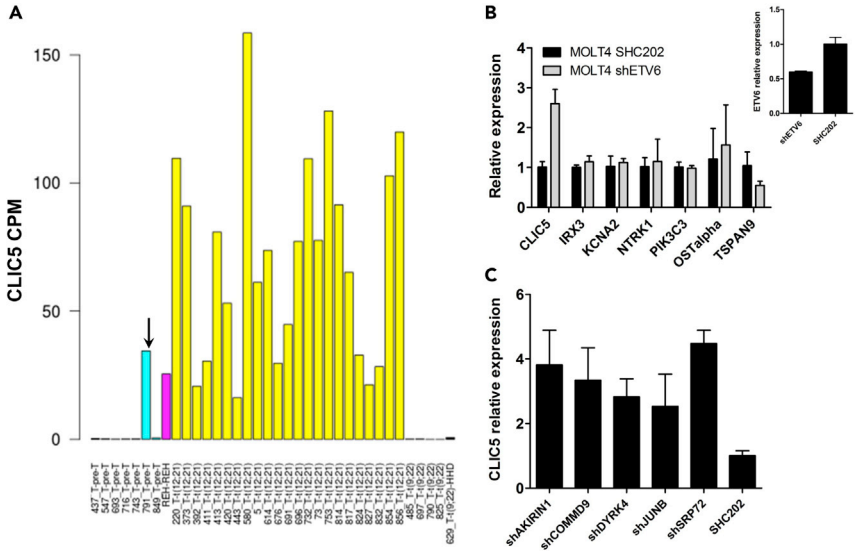

Figure 6. Top *ETV6* modulators in childhood pre-T ALL

(A) Expression of *CLIC5* in leukemic patient samples according to their molecular subtypes. The arrow indicates a pre-T ALL patient with upregulated *CLIC5* expression. Expression in Reh cells is shown for reference (purple).

(B) qRT-PCR analysis of 9 t(12; 21)-associated *ETV6* target genes after shRNA-mediated silencing of *ETV6* in MOLT4 cells (inset). Two of these genes were not expressed (*C6orf222* and *DSC3*; not shown). Data are shown as mean ± SD, n = 6.

(C) Relative expression of *CLIC5* after the knockdown of *ETV6* modulators in MOLT4 cells. Data are shown as mean ± SD, n = 6. See also Figure S4.

upregulation of *CLIC5* in MOLT4 cells (Figure 6C) without any marked downregulation of *ETV6* expression (Figure S4). These results strongly support the role of these genes as modulators of *ETV6*-mediated repression and suggest that *ETV6* modulators are conserved in various cellular contexts.

DISCUSSION

ETV6 loss of function is a key event in the development of hematological malignancies (Moriyama et al., 2015; Noetzli et al., 2015; Topka et al., 2015; Zhang et al., 2015; Bohlander, 2005). To better understand the *ETV6*-mediated repression process we conducted a functional genome-wide shRNA screen. We uncovered 13 novel putative ETV6 modulator genes Including *AKIRIN1*, *COMMD9*, *DYRK4*, *JUNB*, and *SRP72* that demonstrated a broad impact on the *ETV6* transcriptional network in leukemic cells. Alterations in such modulators could disrupt *ETV6* function and participate in hematological diseases.

While the mechanisms of action of these regulators in *ETV6*-mediated transcription remain to be established, several lines of evidence regarding their role in transcriptional regulation are worth mentioning. *AKIRIN1* impact on gene expression was highly restricted to *ETV6* targets, either suggesting an alternative function in human cells or an *ETV6*-specific chromatin remodeling activity. *AKIRIN1* function in human cells remains largely unknown, but it had been found to participate in transcription-associated chromatin remodeling in *Drosophila melanogaster* (Nowak et al., 2012; Bonnay et al., 2014). *COMMD9* was recently associated with *TFDP1*/*E2F1* transcriptional activity in lung cancer (Zhan et al., 2017), suggesting a role in transcription regulation. Moreover, two other COMMD genes, *COMMD8* and *COMMD10*, were also retrieved from the genome-wide screen with a single shRNA, suggesting that this gene family could be implicated in *ETV6* function. This gene family is known to be involved in NF-κB-mediated regulation of transcription (Bartuzi, et al., 2013). The most significant overexpression of *ETV6* target genes was observed when *DYRK4* was knocked down. *DYRK4* is the least studied member of the serine/threonine dual-specificity kinase family (Papadopoulos et al., 2011; Becker et al., 1998) and no role in transcriptional regulation had been associated with this gene so far. Notably, another member of this family, *DYRK3*, was also identified in the primary shRNA screen. DYRK3 phosphorylates histone H2B (Becker et al., 1998) and *SIRT1*, a protein deacetylase that targets histones and other transcription factors such as *E2F1* and NF-κB (Guo et al., 2010). This suggests that SIRT-mediated histone deacetylation could contribute to *ETV6* gene

repression. This is also supported by the capture of shRNAs against *SIRT3* and *SIRT4* in the primary screen. *ETV6* phosphorylation is known to modulate its transcriptional function (Lopez et al., 2003; Poirel et al., 1997; Arai et al., 2002). Thus, *DYRK3* and *DYRK4* could be involved in this process. Determining whether these kinases directly phosphorylate *ETV6*, its modulators or participate in *ETV6*-mediated repression through histones modifications would be of great interest because of their substantial impact on *ETV6* function. *JUNB*, a subunit of the AP-1 transcription factor, is an *ETV6* modulator that was studied in the context of multiple lymphoid malignancies such as lymphomas and T-cell leukemias (Papoudou-Bai et al., 2016). *FOSL2*, another subunit of AP-1, was also captured on the screen with a single shRNA, suggesting that AP-1 participates in the *ETV6* function. Although ETV6 binding to AP-1 was never tested, physical interactions between ETS and AP-1 factors have been described (Bassuk and Leiden, 1995; Verger and Duterque-Coquillaud, 2002). These interactions were dependent on the conserved ETS domain, suggesting that similar interactions could occur with *ETV6* and modulate its transcriptional activity.

In regard to hematological diseases, *SRP72* is an interesting *ETV6* modulator. One of our t(12; 21) negative patient samples showed a 50% reduction in *SRP72* expression compared to other patients, suggesting a monoallelic expression. Expression of the *ETV6* target *OSTalpha* was also significantly higher in this leukemia patient, further supporting that *SRP72* downregulation impacts *ETV6* repressive function. Mutations in *SRP72* have been linked to familial Aplastic Anemia (AA) and Myelodysplasia (MDS) (Kirwan et al., 2012), both of which are also associated with *ETV6* mutations or deletions (Topka et al., 2015). The mechanism(s) through which *SRP72* mutations induce these familial forms of aplasia remains unknown but, considering our findings, could involve the deregulation of *ETV6* target genes. In addition to *SRP72*, *SRP14* was also found with a single shRNA in the genome-wide screen. Furthermore, *SRP9* was identified as an *ETV6*-bound protein by a proteomic approach (Table S4). Altogether, these results suggest that a complex containing SRP proteins could bind *ETV6* to regulate its transcriptional output. SRP proteins' canonical function is to form a complex that binds nascent peptide signals, induce translational arrest, and transfer the ribosomes to the translocon onto the ER where the translation would resume (Akopian et al., 2013). However, we show that *SRP72* silencing does not affect *ETV6* protein level and localization, suggesting an alternate pathway in *ETV6*-mediated repression.

We showed that *ETV6* targets were not equally affected by these modulators. For instance, *DSC3*, a gene significantly repressed by *ETV6* and overexpressed in patients with t(12; 21) positive leukemic, was not significantly influenced by *ETV6* modulators while *OSTalpha, another ETV6 target was* regulated by nine of the 13 modulators. *ETV6* association with certain modulators could be important to regulate specific transcriptional responses following a given signal. For instance, *SEMA3A* and *SEMA3D*, two members of the Semaphorins Class III gene family, are both regulated by *ETV6* and the modulators. The specificity given to *ETV6* by its modulators could ensure that genes belonging to a particular pathway are adequately co-expressed. This suggests that *ETV6* target genes associated with one or more modulators contribute to a common pathway.

Aside from *ETV6* modulators and the chromatin context, other factors might contribute to *ETV6* specificity. For instance, the ETV6-AML1 fusion protein is known to interact with residual *ETV6*, modulate its binding, and dictate specificity (Gunji et al., 2004). In this regard, the expression of *NTRK1*, one of the *ETV6* targets was increased rather than downregulated following the silencing of *ETV6* modulators. Interestingly, *NTRK1* does not contain the *ETV6* consensus binding site(Neveu et al., 2018), suggesting that *ETV6* acts as a co-repressor at this locus. Thus, ETV6-AML1 or other repressive ETS factors (Mavrothalassitis and Ghysdael, 2000) might endogenously repress *NTRK1*. Because ETV6-AML1 retains both the PD and repression domains of *ETV6* and the repressive ETS factors share a similar DNA-binding domain (Kar and Gutierrez-Hartmann, 2013), the identified modulators could affect their repressive function as well, explaining *NTRK1* upregulation following the silencing of *ETV6* modulators. This is of great interest as *ETV6* is involved in multiple translocations with various fusion partners (De Braekeleer et al., 2012) and that ETS factors are widely involved in human malignancies (Ciau-Uitz et al., 2013; Kar and Gutierrez-Hartmann, 2013; Feng et al., 2014; Sizemore et al., 2017). Additional experiments are needed to determine the implication of the novel *ETV6* modulators on other related proteins. In this study, *ETV6* repressive function has been interrogated through a specifically designed functional genome-wide shRNA screen. The individual assessment of a large number of putative modulators and their impact on the *ETV6* transcriptional network unveiled the complexity of *ETV6*-mediated repression. Thirteen novel putative modulators of *ETV6* activity were identified and associated with the regulation of *ETV6* target genes in various contexts. Most of the modulators were involved in a target-specific manner, but some had a broader impact on the *ETV6* transcriptional network. The critical role of *AKIRIN1*, *COMMD9*, *DYRK4*, *JUNB*, and *SRP72* on *ETV6*-mediated regulation

makes them interesting genes regarding the etiology of hematological diseases. Overall, this genome-wide functional screen identified important ETV6 modulators and linked them to the ETV6 transcriptional network.

Limitation of the study

This study focuses on the development and analyses of a genome-wide shRNA screen to identify ETV6 modulators. The screen is a fitness assay taking advantage of a specifically developed ETV6-dependent Blasticidin sensitive cell line. The validation of the modulator was achieved in cellular models but the specific roles of the modulators in ALL as well as in other cancers would need further investigation using patients' samples. The ETV6-RUNX1-like subtype has a similar expression profile to the ETV6-RUNX1 subtype, without the characteristic t(12; 21) translocation, it would thus be interesting to investigate modulators in this subtype. Although our analysis did not reveal a drastic change in the expression levels of the modulators between the two subtypes (Figure S3), a more in-depth analysis accounting for residual ETV6 expression might reveal further insight on their functions.

STAR★METHODS

Detailed methods are provided in the online version of this paper and include the following:

- KEY RESOURCES TABLE
- RESOURCE AVAILABILITY
  - Lead contact
  - Materials availability
  - Data and code availability
- EXPERIMENTAL MODEL AND SUBJECT DETAILS
  - Cell lines
- METHOD DETAILS
  - Establishment and control of the screening cell line
  - Recombinant DNA
  - Lentiviral production and transduction
  - Establishment and control of the screening cell line
  - shRNAs library
  - Genome wide shRNA screening
  - Data analysis
  - Validation of candidate shRNAs by targeted RNA sequencing
  - Targeted RNA sequencing analysis
  - Protein extraction
  - Western blotting
  - Mass spectrometry
  - Database searching
  - Criteria for protein identification
  - qRT-PCR
  - Transcriptome analysis of cancer patients
- QUANTIFICATION AND STATISTICAL

SUPPLEMENTAL INFORMATION

Supplemental information can be found online at https://doi.org/10.1016/j.isci.2022.103858.

ACKNOWLEDGMENTS

Next-generation sequencing was performed at the Integrated Clinical Genomic Center in Pediatrics at the CHU Sainte-Justine Research Center. LC-MS/MS samples were run and analyzed at the Proteomics Platform of the CHU de Quebec Research Center, Quebec, Canada. Computations were performed on the Briarée supercomputer at the Université de Montréal, managed by Calcul Québec and Compute Canada. The operation of this supercomputer is funded by the Canada Foundation for Innovation (CFI), NanoQuébec, RMGA, and the Fonds de recherche du Québec - Nature et technologies (FRQNT). This study was supported by research funds provided by the Terry Fox Research Institute and the Canadian Institutes of Health Research. BN is the recipient of a Cole Foundation scholarship. DS holds the François-Karl Viau Research Chair in Pediatric Oncogenomics.

AUTHOR CONTRIBUTIONS

DS and SG are co-principal investigators and share primary responsibility for the article. BN, CR, SG, and DS contributed to the conception and design of the study. BN, CR, and PC performed most of the experiments. MC analyzed the patients and TCGA expression data. CJC generated the data from the MOLT4 cell line. PSO was involved in the processing of the sequencing data. CF performed some of the Western blots. NG contributed to setting up the genome-wide shRNA screening approach. BN performed data integration and analyses. BN, CR, SG, and DS contributed to data interpretation. BN drafted the article and SG and DS were involved in the critical revision of the article. All authors approved the final version.

DECLARATION OF INTERESTS

The authors declare no competing interests.

B.N. current affiliation: Molecular Diagnostic Laboratory, Montreal Heart Institute, Montreal, Quebec, Canada.

P.C. current affiliations: Program in Infectious Diseases and Global Health, The Research Institute of the McGill University Health Center, Montréal, Quebec, Canada, and McGill International TB Center, Department of Medicine, Faculty of Medicine, McGill University, Montreal, Quebec, Canada.

P.S.O. current affiliation: Center for Integration and Analysis of Medical Data (CITADEL), Department of Medicine, University of Montreal, Center de Recherche du Center Hospitalier de l'Université de Montréal, Montreal, Canada.

N.G current affiliation: Patient Advocacy Lead, Global Product Development, Pfizer Rare Disease, Philadelphia, PA, USA.

D.S is also Scientific Director of CIUSSS du Nord-de-l'Île-de-Montréal (integrated university health and social services centers), Montreal, Canada.

Received: August 13, 2021
Revised: January 1, 2022
Accepted: January 28, 2022
Published: March 18, 2022

REFERENCES

Agape, P., Gerard, B., Cave, H., Devaux, I., Vilmer, E., Lecomte, M.C., and Grandchamp, B. (1997). Analysis of ETV6 and ETV6-AML1 proteins in acute lymphoblastic leukaemia. Br. J. Haematol. *98*, 234–239.

Akopian, D., Shen, K., Zhang, X., and Shan, S.O. (2013). Signal recognition particle: an essential protein-targeting machine. Annu. Rev. Biochem. *82*, 693–721.

Andreasson, P., Schwaller, J., Anastasiadou, E., Aster, J., and Gilliland, D.G. (2001). The expression of ETV6/CBFA2 (TEL/AML1) is not sufficient for the transformation of hematopoietic cell lines in vitro or the induction of hematologic disease in vivo. Cancer Genet. Cytogenet. *130*, 93–104.

Arai, H., Maki, K., Waga, K., Sasaki, K., Nakamura, Y., Imai, Y., Kurokawa, M., Hirai, H., and Mitani, K. (2002). Functional regulation of TEL by p38-induced phosphorylation. Biochem. Biophys. Res. Commun. *299*, 116–125.

Azlan, A., Dzaki, N., and Azzam, G. (2016). Argonaute: the executor of small RNA function. J. Genet. Genomics *43*, 481–494.

Bartuzi, P., Hofker, M.H., and van de Sluis, B. (2013). Tuning NF-kappaB activity: a touch of COMMD proteins. Biochim. Biophys. Acta *1832*, 2315–2321.

Bassuk, A.G., and Leiden, J.M. (1995). A direct physical association between ETS and AP-1 transcription factors in normal human T cells. Immunity *3*, 223–237.

Becker, W., Weber, Y., Wetzel, K., Eirmbter, K., Tejedor, F.J., and Joost, H.G. (1998). Sequence characteristics, subcellular localization, and substrate specificity of DYRK-related kinases, a novel family of dual specificity protein kinases. J. Biol. Chem. *273*, 25893–25902.

Bhojwani, D., Yang, J.J., and Pui, C.H. (2015). Biology of childhood acute lymphoblastic leukemia. Pediatr. Clin. North Am. *62*, 47–60.

Bitterman, K.J., Anderson, R.M., Cohen, H.Y., Latorre-Esteves, M., and Sinclair, D.A. (2002). Inhibition of silencing and accelerated aging by nicotinamide, a putative negative regulator of yeast sir2 and human SIRT1. J. Biol. Chem. *277*, 45099–45107.

Bohlander, S.K. (2005). ETV6: a versatile player in leukemogenesis. Semin. Cancer Biol. *15*, 162–174.

Bonnay, F., Nguyen, X.H., Cohen-Berros, E., Troxler, L., Batsche, E., Camonis, J., Takeuchi, O., Reichhart, J.M., and Matt, N. (2014). Akirin specifies NF-kappaB selectivity of Drosophila innate immune response via chromatin remodeling. EMBO J. *33*, 2349–2362.

Ciau-Uitz, A., Wang, L., Patient, R., and Liu, F. (2013). ETS transcription factors in hematopoietic stem cell development. Blood Cells Mol. Dis. *51*, 248–255.

De Braekeleer, E., Douet-Guilbert, N., Morel, F., Le Bris, M.J., Basinko, A., and De Braekeleer, M. (2012). ETV6 fusion genes in hematological malignancies: a review. Leuk. Res. *36*, 945–961.

Eisenberg, E., and Levanon, E.Y. (2013). Human housekeeping genes, revisited. Trends Genet. *29*, 569–574.

Feng, F.Y., Brenner, J.C., Hussain, M., and Chinnaiyan, A.M. (2014). Molecular pathways:

targeting ETS gene fusions in cancer. Clin. Cancer Res. *20*, 4442–4448.

Golub, T.R., Barker, G.F., Bohlander, S.K., Hiebert, S.W., Ward, D.C., Bray-Ward, P., Morgan, E., Raimondi, S.C., Rowley, J.D., and Gilliland, D.G. (1995). Fusion of the TEL gene on 12p13 to the AML1 gene on 21q22 in acute lymphoblastic leukemia. Proc. Natl. Acad. Sci. U S A. *92*, 4917–4921.

Gu, Z., Churchman, M.L., Roberts, K.G., Moore, I., Zhou, X., Nakitandwe, J., Hagiwara, K., Pelletier, S., Gingras, S., Berns, H., et al. (2019). PAX5-driven subtypes of B-progenitor acute lymphoblastic leukemia. Nat. Genet. *51*, 296–307.

Guidez, F., Petrie, K., Ford, A.M., Lu, H., Bennett, C.A., MacGregor, A., Hannemann, J., Ito, Y., Ghysdael, J., Greaves, M., et al. (2000). Recruitment of the nuclear receptor corepressor N-CoR by the TEL moiety of the childhood leukemia-associated TEL-AML1 oncoprotein. Blood *96*, 2557–2561.

Gunji, H., Waga, K., Nakamura, F., Maki, K., Sasaki, K., Nakamura, Y., and Mitani, K. (2004). TEL/AML1 shows dominant-negative effects over TEL as well as AML1. Biochem. Biophys. Res. Commun. *322*, 623–630.

Guo, X., Williams, J.G., Schug, T.T., and Li, X. (2010). DYRK1A and DYRK3 promote cell survival through phosphorylation and activation of SIRT1. J. Biol. Chem. *285*, 13223–13232.

Hart, T., Komori, H.K., LaMere, S., Podshivalova, K., and Salomon, D.R. (2013). Finding the active genes in deep RNA-seq gene expression studies. BMC Genomics *14*, 778.

Kar, A., and Gutierrez-Hartmann, A. (2013). Molecular mechanisms of ETS transcription factor-mediated tumorigenesis. Crit. Rev. Biochem. Mol. Biol. *48*, 522–543.

Kirwan, M., Walne, A.J., Plagnol, V., Velangi, M., Ho, A., Hossain, U., Vulliamy, T., and Dokal, I. (2012). Exome sequencing identifies autosomal-dominant SRP72 mutations associated with familial aplasia and myelodysplasia. Am. J. Hum. Genet. *90*, 888–892.

Kuwata, T., Gongora, C., Kanno, Y., Sakaguchi, K., Tamura, T., Kanno, T., Basrur, V., Martinez, R., Appella, E., Golub, T., and Ozato, K. (2002). Gamma interferon triggers interaction between ICSBP (IRF-8) and TEL, recruiting the histone deacetylase HDAC3 to the interferon-responsive element. Mol. Cell Biol. *22*, 7439–7448.

Lajoie, M., Drouin, S., Caron, M., St-Onge, P., Ouimet, M., Gioia, R., Lafond, M.H., Vidal, R., Richer, C., Oualkacha, K., et al. (2017). Specific expression of novel long non-coding RNAs in high-hyperdiploid childhood acute lymphoblastic leukemia. PLoS One *12*, e0174124.

Langmead, B., and Salzberg, S.L. (2012). Fast gapped-read alignment with Bowtie 2. Nat. Methods *9*, 357–359.

Lee, Y.J., Kim, J.H., Bae, S., Rho, S.K., and Choe, S.Y. (2004). Mechanism of transcriptional repression by TEL/RUNX1 fusion protein. Mol. Cells *17*, 217–222.

Lilljebjorn, H., Henningsson, R., Hyrenius-Wittsten, A., Olsson, L., Orsmark-Pietras, C., von Palffy, S., Askmyr, M., Rissler, M., Schrappe, M., Cario, G., et al. (2016). Identification of ETV6-RUNX1-like and DUX4-rearranged subtypes in paediatric B-cell precursor acute lymphoblastic leukaemia. Nat. Commun. *7*, 11790.

Lilljebjorn, H., Soneson, C., Andersson, A., Heldrup, J., Behrendtz, M., Kawamata, N., Ogawa, S., Koeffler, H.P., Mitelman, F., Johansson, B., et al. (2010). The correlation pattern of acquired copy number changes in 164 ETV6/RUNX1-positive childhood acute lymphoblastic leukemias. Hum. Mol. Genet. *19*, 3150–3158.

Livak, K.J., and Schmittgen, T.D. (2001). Analysis of relative gene expression data using real-time quantitative PCR and the 2(-Delta Delta C(T)) Method. Methods *25*, 402–408.

Lopez, R.G., Carron, C., and Ghysdael, J. (2003). v-SRC specifically regulates the nucleo-cytoplasmic delocalization of the major isoform of TEL (ETV6). J. Biol. Chem. *278*, 41316–41325.

Mavrothalassitis, G., and Ghysdael, J. (2000). Proteins of the ETS family with transcriptional repressor activity. Oncogene *19*, 6524–6532.

Montpetit, A., Larose, J., Boily, G., Langlois, S., Trudel, N., and Sinnett, D. (2004). Mutational and expression analysis of the chromosome 12p candidate tumor suppressor genes in pre-B acute lymphoblastic leukemia. Leukemia *18*, 1499–1504.

Mori, H., Colman, S.M., Xiao, Z., Ford, A.M., Healy, L.E., Donaldson, C., Hows, J.M., Navarrete, C., and Greaves, M. (2002). Chromosome translocations and covert leukemic clones are generated during normal fetal development. Proc. Natl. Acad. Sci. U S A. *99*, 8242–8247.

Moriyama, T., Metzger, M.L., Wu, G., Nishii, R., Qian, M., Devidas, M., Yang, W., Cheng, C., Cao, X., Quinn, E., et al. (2015). Germline genetic variation in ETV6 and risk of childhood acute lymphoblastic leukaemia: a systematic genetic study. Lancet Oncol. *16*, 1659–1666.

Neveu, B., Caron, M., Lagace, K., Richer, C., and Sinnett, D. (2018). Genome wide mapping of ETV6 binding sites in pre-B leukemic cells. Sci. Rep. *8*, 15526.

Neveu, B., Spinella, J.F., Richer, C., Lagace, K., Cassart, P., Lajoie, M., Jananji, S., Drouin, S., Healy, J., Hickson, G.R., and Sinnett, D. (2016). CLIC5: a novel ETV6 target gene in childhood acute lymphoblastic leukemia. Haematologica *101*, 1534–1543.

Noetzli, L., Lo, R.W., Lee-Sherick, A.B., Callaghan, M., Noris, P., Savoia, A., Rajpurkar, M., Jones, K., Gowan, K., Balduini, C.L., et al. (2015). Germline mutations in ETV6 are associated with thrombocytopenia, red cell macrocytosis and predisposition to lymphoblastic leukemia. Nat. Genet. *47*, 535–538.

Nowak, S.J., Aihara, H., Gonzalez, K., Nibu, Y., and Baylies, M.K. (2012). Akirin links twist-regulated transcription with the Brahma chromatin remodeling complex during embryogenesis. PLoS Genet. *8*, e1002547.

Otsubo, K., Kanegane, H., Eguchi, M., Eguchi-Ishimae, M., Tamura, K., Nomura, K., Abe, A., Ishii, E., and Miyawaki, T. (2010). ETV6-ARNT fusion in a patient with childhood T lymphoblastic leukemia. Cancer Genet. Cytogenet. *202*, 22–26.

Papadopoulos, C., Arato, K., Lilienthal, E., Zerweck, J., Schutkowski, M., Chatain, N., Muller-Newen, G., Becker, W., and de la Luna, S. (2011). Splice variants of the dual specificity tyrosine phosphorylation-regulated kinase 4 (DYRK4) differ in their subcellular localization and catalytic activity. J. Biol. Chem. *286*, 5494–5505.

Papoudou-Bai, A., Hatzimichael, E., Barbouti, A., and Kanavaros, P. (2016). Expression patterns of the activator protein-1 (AP-1) family members in lymphoid neoplasms. Clin. Exp. Med. *17*, 291–304.

Patel, N., Goff, L.K., Clark, T., Ford, A.M., Foot, N., Lillington, D., Hing, S., Pritchard-Jones, K., Jones, L.K., and Saha, V. (2003). Expression profile of wild-type ETV6 in childhood acute leukaemia. Br. J. Haematol. *122*, 94–98.

Poirel, H., Lacronique, V., Mauchauffe, M., Le Coniat, M., Raffoux, E., Daniel, M.T., Erickson, P., Drabkin, H., MacLeod, R.A., Drexler, H.G., et al. (1998). Analysis of TEL proteins in human leukemias. Oncogene *16*, 2895–2903.

Poirel, H., Oury, C., Carron, C., Duprez, E., Laabi, Y., Tsapis, A., Romana, S.P., Mauchauffe, M., Le Coniat, M., Berger, R., et al. (1997). The TEL gene products: nuclear phosphoproteins with DNA binding properties. Oncogene *14*, 349–357.

Quinlan, A.R., and Hall, I.M. (2010). BEDTools: a flexible suite of utilities for comparing genomic features. Bioinformatics *26*, 841–842.

Romana, S.P., Mauchauffe, M., Le Coniat, M., Chumakov, I., Le Paslier, D., Berger, R., and Bernard, O.A. (1995a). The t(12;21) of acute lymphoblastic leukemia results in a tel-AML1 gene fusion. Blood *85*, 3662–3670.

Romana, S.P., Poirel, H., Leconiat, M., Flexor, M.A., Mauchauffe, M., Jonveaux, P., Macintyre, E.A., Berger, R., and Bernard, O.A. (1995b). High frequency of t(12;21) in childhood B-lineage acute lymphoblastic leukemia. Blood *86*, 4263–4269.

Samur, M.K. (2014). RTCGAToolbox: a new tool for exporting TCGA Firehose data. PLoS One *9*, e106397.

Sanders, B.D., Jackson, B., and Marmorstein, R. (2010). Structural basis for sirtuin function: what we know and what we don't. Biochim. Biophys. Acta *1804*, 1604–1616.

Schmidt, M.T., Smith, B.C., Jackson, M.D., and Denu, J.M. (2004). Coenzyme specificity of Sir2 protein deacetylases: implications for physiological regulation. J. Biol. Chem. *279*, 40122–40129.

Shurtleff, S.A., Buijs, A., Behm, F.G., Rubnitz, J.E., Raimondi, S.C., Hancock, M.L., Chan, G.C., Pui, C.H., Grosveld, G., and Downing, J.R. (1995). TEL/AML1 fusion resulting from a cryptic t(12;21) is the most common genetic lesion in pediatric ALL and defines a subgroup of patients with an excellent prognosis. Leukemia *9*, 1985–1989.

Singh, R., Park, D., Xu, J., Hosur, R., and Berger, B. (2010). Struct2Net: a web service to predict protein-protein interactions using a structure-based approach. Nucleic Acids Res. *38*, W508–W515.

Sizemore, G.M., Pitarresi, J.R., Balakrishnan, S., and Ostrowski, M.C. (2017). The ETS family of oncogenic transcription factors in solid tumours. Nat. Rev. Cancer *17*, 337–351.

Spinella, J.F., Cassart, P., Richer, C., Saillour, V., Ouimet, M., Langlois, S., St-Onge, P., Sontag, T., Healy, J., Minden, M.D., and Sinnett, D. (2016). Genomic characterization of pediatric T-cell acute lymphoblastic leukemia reveals novel recurrent driver mutations. Oncotarget *7*, 65485–65503.

Szymczyna, B.R., and Arrowsmith, C.H. (2000). DNA binding specificity studies of four ETS proteins support an indirect read-out mechanism of protein-DNA recognition. J. Biol. Chem. *275*, 28363–28370.

Topka, S., Vijai, J., Walsh, M.F., Jacobs, L., Maria, A., Villano, D., Gaddam, P., Wu, G., McGee, R.B., Quinn, E., et al. (2015). Germline ETV6 mutations confer susceptibility to acute lymphoblastic leukemia and thrombocytopenia. Plos Genet. *11*, e1005262.

Trapnell, C., Williams, B.A., Pertea, G., Mortazavi, A., Kwan, G., van Baren, M.J., Salzberg, S.L., Wold, B.J., and Pachter, L. (2010). Transcript assembly and quantification by RNA-Seq reveals unannotated transcripts and isoform switching during cell differentiation. Nat. Biotechnol. *28*, 511–515.

Uphoff, C.C., MacLeod, R.A., Denkmann, S.A., Golub, T.R., Borkhardt, A., Janssen, J.W., and Drexler, H.G. (1997). Occurrence of TEL-AML1 fusion resulting from (12;21) translocation in human early B-lineage leukemia cell lines. Leukemia *11*, 441–447.

van der Weyden, L., Giotopoulos, G., Rust, A.G., Matheson, L.S., van Delft, F.W., Kong, J., Corcoran, A.E., Greaves, M.F., Mullighan, C.G., Huntly, B.J., and Adams, D.J. (2011). Modeling the evolution of ETV6-RUNX1-induced B-cell precursor acute lymphoblastic leukemia in mice. Blood *118*, 1041–1051.

Verger, A., and Duterque-Coquillaud, M. (2002). When Ets transcription factors meet their partners. Bioessays *24*, 362–370.

Wang, L., and Hiebert, S.W. (2001). TEL contacts multiple co-repressors and specifically associates with histone deacetylase-3. Oncogene *20*, 3716–3725.

Yeoh, E.J., Ross, M.E., Shurtleff, S.A., Williams, W.K., Patel, D., Mahfouz, R., Behm, F.G., Raimondi, S.C., Relling, M.V., Patel, A., et al. (2002). Classification, subtype discovery, and prediction of outcome in pediatric acute lymphoblastic leukemia by gene expression profiling. Cancer Cell *1*, 133–143.

Zhan, W., Wang, W., Han, T., Xie, C., Zhang, T., Gan, M., and Wang, J.B. (2017). COMMD9 promotes TFDP1/E2F1 transcriptional activity via interaction with TFDP1 in non-small cell lung cancer. Cell Signal *30*, 59–66.

Zhang, M.Y., Churpek, J.E., Keel, S.B., Walsh, T., Lee, M.K., Loeb, K.R., Gulsuner, S., Pritchard, C.C., Sanchez-Bonilla, M., Delrow, J.J., et al. (2015). Germline ETV6 mutations in familial thrombocytopenia and hematologic malignancy. Nat. Genet. *47*, 180–185.

STAR★METHODS

KEY RESOURCES TABLE

REAGENT or RESOURCE	SOURCE	IDENTIFIER
Antibodies		
Anti-ETV6 / Tel antibody	Abcam	Cat# ab54705; RRID: AB_941491
GAPDH Antibody (L-20)	Santa Cruz Biotechnology	Cat# sc-31915; RRID: AB_641105
Anti-β-Actin Antibody (ACTBD11B7)	Santa Cruz Biotechnology	Cat# sc-81178; RRID: AB_2223230
Recombinant Anti-PCNA antibody [EPR3821]	Abcam	Cat# ab92552; RRID: AB_10561973
Bacterial and virus strains		
Mission TRC shRNA whole library	Sigma-Aldrich	CP0001 55K Human Pool + CP0003 90K Human Pool
Critical commercial assays		
Pierce™ Anti-HA Magnetic Beads	Thermo Fisher	Cat# 88836; RRID: AB_2861399
Deposited data		
RNA-seq data	(Neveu et al., 2016)	GEO: GSE79373
ChIP-seq data	(Neveu et al., 2018)	GEO: GSE102785
LC-MS/MS data	This study	ProteomeXchange: PXD031001
Experimental models: Cell lines		
REH	ATCC	Cat# CRL-8286; RRID: CVCL_1650
HEK293T	ATCC	Cat# CRL-11268; RRID: CVCL_0063
Reh BlastR 2-1	This study	N/A
2-1 ETV6-5	This study	N/A
MOLT4	ATCC	Cat# CRL-1582; RRID: CVCL_001
Oligonucleotides		
All primer sequences are listed in Table S5		
Recombinant DNA		
pLENTI CMV TetR Blast	Addgene	Cat# 17492; RRID: Addgene_17492
pENTR3C	Invitrogen	11817-012
pGL4 EBS_3tk BlastR	This study	N/A
pGL3 EBS3tk	This study	N/A
pLENTI CMV puro DEST (w118-1)	Dr. Christian Beauséjour, CHU Sainte-Justine, Montreal, QC, Canada	Addgene #17452; RRID: Addgene_17452
pLENTI ETV6	This study	N/A
pcDNA3.1 ETV6	(Neveu et al., 2018)	N/A
pCCL ETV6-HA	(Neveu et al., 2018)	N/A
pCCL ETV6	(Neveu et al., 2018)	N/A
Software and algorithms		
GraphPad Prism 5	GraphPad Software	https://www.graphpad.com/ RRID:SCR_002798
Cufflinks tool version 2.2.1	(Trapnell et al., 2010)	https://github.com/cole-trapnell-lab/cufflinks RRID:SCR_014597
Bowtie2	(Langmead and Salzberg, 2012)	https://github.com/BenLangmead/bowtie2 RRID:SCR_016368

(*Continued on next page*)

Continued

REAGENT or RESOURCE	SOURCE	IDENTIFIER
BEDTools version 2.22.1.	(Quinlan and Hall, 2010)	https://github.com/arq5x/bedtools2 RRID:SCR_006646
RTCGAToolbox v.2.0.0	(Samur, 2014)	https://bioconductor.org/packages/release/bioc/html/RTCGAToolbox.html
Mascot version 2.5.1	Matrix Science	https://www.matrixscience.com/ RRID:SCR_014322
Scaffold version 5.0.1	Proteome Software Inc.	https://www.proteomesoftware.com/products/scaffold-5 RRID:SCR_014345

RESOURCE AVAILABILITY

Lead contact

Further information and requests for resources and reagents should be directed to and will be fulfilled by the lead contact, Daniel Sinnett (daniel.sinnett@umontreal.ca).

Materials availability

All requests for resources and reagents should be directed to and will be fulfilled by the lead contact, Daniel Sinnett (daniel.sinnett@umontreal.ca). All reagents will be made available on request after completion of a Materials Transfer Agreement.

Data and code availability

- The RNA-seq and ChIP-seq data used in this study have been deposited in NCBI's Gene Expression Omnibus and are accessible through GEO Series accession number GSE79373 and GSE102785 respectively. The mass spectrometry proteomics data have been deposited to the ProteomeXchange Consortium via the PRIDE partner repository with the dataset identifier PXD031001.
- This paper does not report original code.
- Any additional information required to reanalyze the data reported in this paper is available from the lead contact upon request.

EXPERIMENTAL MODEL AND SUBJECT DETAILS

Cell lines

The Reh (ATCC, Manassas, VA, USA, CRL-8286) cell line and derived clones were maintained in RPMI 1640 (Wisent, Saint-Bruno, QC, Canada) 10% Fetal Bovine Serum (FBS; Wisent, Saint-Bruno, QC, Canada) in a 5% CO_2 incubator at 37°C. The MOLT4 (ATCC, CRL-1582) cell line and derived clones were maintained in RPMI 1640 (Wisent, Saint-Bruno, QC, Canada) 10% Fetal Bovine Serum (FBS; Wisent, Saint-Bruno, QC, Canada) in a 5% CO_2 incubator at 37°C.

METHOD DETAILS

Establishment and control of the screening cell line

The Reh (ATCC, Manassas, VA, USA, CRL-8286) cell line and derived clones were maintained in RPMI 1640 (Wisent, Saint-Bruno, QC, Canada) 10% Fetal Bovine Serum (FBS; Wisent, Saint-Bruno, QC, Canada) in a 5% CO_2 incubator at 37°C. Reh cells were transfected with pGL4 EBS_3tk BlastR using the Lipofectamine 2000 reagent (Thermo Fisher Scientific, Waltham, MA, USA). Media was changed the next day and 2 μg/mL Blasticidin was added 48h post-transfection for selection. Cells were maintained for a month under Blasticidin selective pressure to retrieve cells with a stable integration. Using 6-wells plates, 500 cells from this Blasticidin resistant population were seeded in 1 mL of MethoCult H4230 media (STEMCELL Technologies, Vancouver, BC, Canada) containing 2 μg/mL Blasticidin and grown for an additional month to obtain distinct colonies (clones). Colonies were transferred and amplified in 96-wells liquid cultures with 2 μg/mL Blasticidin. Blasticidin resistant clones were then transduced with pLENTI *ETV6* or pLENTI empty vector lentiviral particles. Cells were selected with 1 μg/mL puromycin before assessing *ETV6* and BlastR

expression by quantitative real-time PCR (qRT-PCR; see related section). The selected clone (Reh EBS_3tk BlastR 2-1) was submitted to an additional round of clonal selection in methylcellulose media (1 μg/mL puromycin) to ensure a strict and homogenous cellular system with single EBS_3tk BlastR and *ETV6* integrations (i.e. Reh EBS_3tk BlastR 2-1 ETV6-5).

A GFP selectable pLKO plasmid containing a shRNA against *ETV6* (shETV6) was used for lentiviral production and transduction of the *ETV6*-dependent Blasticidin sensitive clone 2-1 ETV6-5. A scrambled shRNA sequence ($shCtl^{ETV6}$) was also included as a negative control. GFP positive cells were retrieved by flow cytometry using the FACSAria IIu cell sorter (Becton Dickinson, Franklin Lakes, NJ, USA) and stabilized in culture for several days before validating the *ETV6* knockdown by Western Blotting and qRT-PCR (see related sections). GFP positive cells were seeded at an initial concentration of 1×10^5 cells/mL and treated with a range of Blasticidin doses (5,10 and 25 μg/mL). Cells were then cultured for 12 days in these conditions and proliferation was evaluated with the Z1 Particle Counter (Beckman Coulter, Brea, CA, USA). Alternatively, both the original Reh EBS_3tk BlastR 2-1 clone and the *ETV6* expressing 2-1 ETV6-5 clone were treated with Nicotinamide (NAM; Sigma-Aldrich, Saint Louis, MO, USA) at a final concentration of 20 mM for 72h. BlastR expression was then evaluated by qRT-PCR (see related section).

Recombinant DNA

pGL4 EBS_3tk BlastR plasmid was constructed by cloning PCR products of the Blasticidin résistance gene (BlastR) from pLENTI CMV TetR Blast (716-1) plasmid (Addgene, Watertown, MA, USA) between the NcoI and Xba restriction sites and the EBS_3tk artificial promoter from the pGL3 EBS_3tk vector between the KpnI and NheI restriction sites.

The complete *ETV6* complementary DNA (cDNA) sequence (NM_001987) obtained from pcDNA3.1 *ETV6* (Neveu et al., 2018) was subcloned into the Gateway compatible vector pENTR 3C and transferred into the pLENTI CMV puro DEST (w118-1) lentiviral vector (kindly provided by Dr. Christian Beauséjour) using LR clonase II reactions according to the manufacturer protocol (Thermo Fisher Scientific, Waltham, MA, USA).

Lentiviral production and transduction

Production of lentiviral particles and cell transduction were performed as previously described (Neveu et al., 2016). Briefly, HEK293T cells (ATCC, CRL-11268) were transfected with the lentiviral expression plasmid (pLENTI backbone) together with the third generation encapsidation plasmids, pRSV-Rev, pMD2.VSVG and pMDL (kindly provided by Dr. Christian Beauséjour) using Polyethylenimine (Polysciences). Media was renewed 16h post-transfection and cells were cultured for 30h. Viral particles from culture media were concentrated by ultracentrifugation (50 000 g) and estimated using the p24 antigen ELISA (Advanced Bioscience Laboratories). The transduction was performed by adding these particles (10-100 ng per 1×10^5 cells) and 8 μg/mL polybrene (Sigma-Aldrich, Saint Louis, MO, USA) to cells for 24h. Media was changed and the selection agent (i.e. 1 μg/mL puromycin) was added 48h post-transduction. Cells were cultured for at least 2 weeks prior to any experiments. (*refer to the ''shRNAs preparation'' section for the pLKO shRNAs particles.)*

Establishment and control of the screening cell line

The Reh (ATCC, Manassas, VA, USA, CRL-8286) cell line and derived clones were maintained in RPMI 1640 (Wisent, Saint-Bruno, QC, Canada) 10% Fetal Bovine Serum (FBS; Wisent, Saint-Bruno, QC, Canada) in a 5% CO_2 incubator at 37°C. Reh cells were transfected with pGL4 EBS_3tk BlastR using the Lipofectamine 2000 reagent (Thermo Fisher Scientific, Waltham, MA, USA). Media was changed the next day and 2 μg/mL Blasticidin was added 48h post-transfection for selection. Cells were maintained for a month under Blasticidin selective pressure to retrieve cells with a stable integration. Using 6-wells plates, 500 cells from this Blasticidin resistant population were seeded in 1 mL of MethoCult H4230 media (STEMCELL Technologies, Vancouver, BC, Canada) containing 2 μg/mL Blasticidin and grown for an additional month to obtain distinct colonies (clones). Colonies were transferred and amplified in 96-wells liquid cultures with 2 μg/mL Blasticidin. Blasticidin resistant clones were then transduced with pLENTI *ETV6* or pLENTI empty vector lentiviral particles. Cells were selected with 1 μg/mL puromycin before assessing *ETV6* and BlastR expression by quantitative real-time PCR (qRT-PCR; see related section). The selected clone (Reh EBS_3tk BlastR 2-1) was submitted to an additional round of clonal selection in methylcellulose media (1 μg/mL puromycin) to ensure a strict and homogenous cellular system with single EBS_3tk BlastR and *ETV6* integrations (i.e. Reh EBS_3tk BlastR 2-1 ETV6-5).

A GFP selectable pLKO plasmid containing a shRNA against *ETV6* (shETV6) was used for lentiviral production and transduction of the *ETV6*-dependent Blasticidin sensitive clone 2-1 ETV6-5. A scrambled shRNA sequence ($shCtl^{ETV6}$) was also included as a negative control. GFP positive cells were retrieved by flow cytometry using the FACSAria IIu cell sorter (Becton Dickinson, Franklin Lakes, NJ, USA) and stabilized in culture for several days before validating the *ETV6* knockdown by Western Blotting and qRT-PCR (see related sections). GFP positive cells were seeded at an initial concentration of 1×10^5 cells/mL and treated with a range of Blasticidin doses (5,10 and 25 μg/mL). Cells were then cultured for 12 days in these conditions and proliferation was evaluated with the Z1 Particle Counter (Beckman Coulter, Brea, CA, USA). Alternatively, both the original Reh EBS_3tk BlastR 2-1 clone and the *ETV6* expressing 2-1 ETV6-5 clone were treated with Nicotinamide (NAM; Sigma-Aldrich, Saint Louis, MO, USA) at a final concentration of 20 mM for 72h. BlastR expression was then evaluated by qRT-PCR (see related section).

shRNAs library

Lentiviral particles were prepared from the Mission TRC shRNA whole library (Sigma-Aldrich, Saint Louis, MO, USA) according to the manufacturer's protocol. Briefly, the library was divided in 15 pools each containing approximately 9600 different shRNAs (10 96-well plates/pool). For lentiviral production, HEK293T cells were transfected (FuGENE 6, Promega, Madison, WI, USA) with the shRNA plasmid pools, psPAX2 (Addgene, Watertown, MA, USA) and pMD2.G (Addgene, Watertown, MA, USA) at a ratio of 1/0.75/0.25. Cell culture media were harvested and filtered (0.45 μm filter) 48 h post-transfection. The lentiviral titer of each pool was evaluated by limiting dilution using NIH3T3 cells.

The multiplicity of infection (MOI) of each shRNAs pool was evaluated by transducing Reh cells with various dilutions of viral particles using 5 μg/mL polybrene. The next day, media was replaced, and cells were selected with 1 μg/mL puromycin for 48h. Cell viability was assessed by propidium iodide (PI) staining (final concentration of 0.2 μg/mL in PBS). 1×10^4 stained cells were analyzed by flow cytometry on a LSRFortessa FACS (Becton Dickinson, Franklin Lakes, NJ, USA). Data was acquired with the FACSDiva software (Becton Dickinson, Franklin Lakes, NJ, USA).

For individual shRNAs, HEK293T cells were transfected with the pLKO shRNA construct together with the third generation encapsidation plasmids, pRSV-Rev, pMD2.VSVG and pMDL using Lipofectamine 2000 (Thermo Fisher Scientific, Waltham, MA, USA). Media was renewed 16h post-transfection and harvested after an additional 30h of culture. Viral particles were used directly for transduction.

Genome wide shRNA screening

1×10^7 *ETV6*-dependent Blasticidin sensitive 2-1 ETV6-5 cells were transduced with each of the 15 shRNAs pools at a MOI of 0.3-0.4 (determined for each pool; see ''*shRNAs preparation*'' section) using 5 μg/mL polybrene. In these conditions, each unique shRNA is expected to be integrated by approximately 200 cells. Media was changed the next day and replaced with fresh media containing 1 μg/mL puromycin. Cells were maintained in culture for 14 days to allow knockdowns to modulate *ETV6* function and BlastR expression. Each pool of cells was then split into 3 parts: 1×10^7 cells were pelleted and used as the initial time point of the experiment (T_{14}), 2×10^7 cells were maintained as is (no Blasticidin), and 5×10^7 cells were treated with 50 μg/mL Blasticidin. After 14 days, 1×10^7 cells of each shRNAs pool (with and without Blasticidin selection) were pelleted and used as the first time point of selection (T_{28}). Cells were maintained for an additional 14 days in culture in these conditions and pellets were taken for each shRNA pool and used as the final time point of selection (T_{42}).

Genomic DNA (gDNA) was extracted from each sample using the QIAamp DNA Mini Kit according to the manufacturer's protocol (Qiagen, Hilden, Germany). Quantification was performed on Qubit using the Quant-it PicoGreen dsDNA Kit (Broad range; Thermo Fisher Scientific, Waltham, MA, USA). 6 μg of gDNA was used as template for the first PCR with primers flanking the integrated shRNA sequences and containing Illumina-compatible overhang extremities: F- TCGTCGGCAGCGTCAGATGTGTATAAGAG ACAGCCGTAACTTGAAAGTATTTCGATTTCTTGGCTTTATATATCTTGTGG; R- GTCTCGTGGGCTCGGA GATGTGTATAAGAGACAGTTGTGGATGAATACTGCCATTTGTCTC. To evaluate the sensitivity of the methodology, duplicates of T_{14} samples were supplemented with respectively 20 and 200 copies of SHC002 and SHC202 lentiviral vectors prior to the first PCR. Technical duplicates for each T_{14} samples also allowed the assessment of the reproducibility of the PCR and sequencing methods. For each sample, 12 amplification reactions of 50 μL were performed as follow: gDNA: 10 ng/uL, primers: 0.25 μM each,

dNTPs: 0.3 mM and 1U KAPA HiFi DNA polymerase (KAPA Biosystems, Wilmington, MA, USA) in 1X KAPA reaction buffer. Thermocycling method: 95°C, 4 min; [98°C, 20 sec; 70°C, 15 sec; 72°C, 1 min] X 15 cycles; 72°C, 5 min. PCR reactions from each gDNA sample were pooled and 90 μL were purified with 1.8X volume AMPure XP magnetic beads (Beckman Coulter, Brea, CA, USA) and eluted in 30 μL water. The second amplification reaction used Nextera XT index Kit v2 primers (Illumina, San Diego, CA, USA) and was performed in 50 μL as follow: purified PCR#1: 30 μL, primers: 5 μL each, dNTPs: 0.3 mM and 1U KAPA HiFi DNA polymerase in 1X KAPA reaction buffer. Thermocycling method: 95°C, 4 min; [98°C, 20 sec; 68°C, 30 sec; 72°C, 30 sec] X 12 cycles; 72°C, 5 min. Reactions were once again purified with AMPure XP magnetic beads (as above). Amplicons size was confirmed by Bioanalyser on a DNA 1000 chip (Agilent Technologies, Santa Clara, CA, USA) and libraries were sequenced using the HiSeq 2500 system (paired-end 100 b. p.; Illumina, San Diego, CA, USA) with 9×10^6 reads per library.

Data analysis

Reads from each sample were aligned on a custom reference containing all the target sequences of the MISSION Human shRNA library using the Bowtie2 alignment tool version 2.2.3 (Langmead and Salzberg, 2012). For a given shRNAs pool and for each condition (T_{14}, T_{28} with and without Blasticidin, T_{42} with and without Blasticidin), read counts per shRNA were obtained using BEDTools version 2.22.1 (Quinlan and Hall, 2010). Note that for T_{14} samples, the technical duplicates were merged at this point. Every shRNA counts in a sample were normalized per the total number of reads in that sample to reflect their relative abundance. shRNAs with no coverage (0) in at least one of the time points were removed from further analyses. To be considered a positive hit, a shRNA had to have a greater normalized count in the Blasticidin condition compared to the untreated control condition at both time points (T_{28} and T_{42}). The normalized count also had to be greater at the end of the experiment (T_{42} with Blasticidin) compared to the initial count at T_{14}. These positive shRNA hits were further refined using additional thresholds. We filtered out weakly over-represented shRNAs ($\sum$Counts(BlastS - ØBlastS) is less than 2 standard deviation of SHC202 control vector; $\leq$ 9,770;) as well as shRNAs which target non-expressed genes (Hart et al., 2013) in Reh cells (Neveu et al., 2016).

Validation of candidate shRNAs by targeted RNA sequencing

The shRNAs selected for validation (Table S2) and two negative controls from the MISSION library (SHC002 and SHC202) were used individually to produce lentiviral particles and transduce Reh *ETV6* cells (as described in the '' shRNAs preparation'' section). All shRNA particles were used at a 1/10 to 1/20 dilution to reach a MOI >1. All shRNA cell lines were maintained with 1 μg/mL puromycin for 2 weeks.

Total RNA was extracted from these shRNA populations using the RNeasy Mini kit (Qiagen, Hilden, Germany). Two biological replicates of Reh *ETV6* cells and one of Reh pLENTI were also included as additional controls. 50 ng of RNA was then processed through the TruSeq Targeted RNA expression kit according to the manufacturer's protocol (Illumina, San Diego, CA, USA). Amplicons included *ETV6* target genes (Neveu et al., 2016), non-*ETV6* target genes (apoptosis panel; Illumina), genes targeted by shRNAs (Table S2) and housekeeping genes (Eisenberg and Levanon, 2013). Amplicons size was confirmed by Bioanalyser on a DNA 1000 chip (Agilent Technologies, Santa Clara, CA, USA). Amplicons were sequenced on a HiSeq 2500 system (paired-end 100 b.p.; Illumina, San Diego, CA, USA) with 1.8×10^6 reads per sample. Mapping was performed using the Illumina BaseSpace SequenceHub Informatics suite and raw counts were obtained and further processed.

Targeted RNA sequencing analysis

Raw counts for each gene in a sample were first normalized per the number of total reads in that sample. Genes considered very weakly expressed (mean normalised counts < 10 and/or normalised pLENTI counts < 10) were discarded from the analyses. Expression in each sample was further normalised using 12 housekeeping genes (Eisenberg and Levanon, 2013). For each gene, the relative expression in each shRNA sample was calculated compared to the SHC002 and SHC202 controls by including the variability of the 4 *ETV6* replicates: ((shRNA sample count - SHC002 and SHC202 mean count) / standard deviation of the 4 *ETV6* controls). The relative expression of a gene was also calculated as a simple ratio against the SHC002 and SHC202 controls: (shRNA sample count / SHC002 and SHC202 mean count). Using standard deviation-corrected relative expressions, shRNAs inducing a specific re-expression of validated *ETV6* targets, but not *ETV6* independent genes, according to a Welch's corrected Student *t* test, were

considered positives. Knockdown efficiency for each shRNA sample was calculated similarly. Heatmaps were generated with the pheatmap R package.

Protein extraction

1×10^7 cells were washed in PBS and disrupted for 15 min on ice in a hypotonic cytoplasm extraction buffer (CEB; 10 mM HEPES pH 7.5, 10mM KCl, 1X Protease Inhibitors Set III Animal-free (Calbiochem, San Diego, CA, USA); 100 µL/1 × 10^7 cells). NP-40 was added to a final concentration of 0.05% prior to centrifugation. Supernatant containing the cytoplasmic proteins was collected and the nuclei pellet was washed in CEB buffer. Nuclei were then disrupted in a hypertonic nuclear extraction buffer (NEB; 20 mM HEPES pH 7.5, 50 mM KCl, 300 mM NaCl, 5% Glycerol, 0.05% NP-40, 1X Protease Inhibitors Set III (with EDTA); 100 µL/1 × 10^7 cells) for 1 hour with agitation at 4°C. The supernatant obtained after centrifugation contained soluble nuclear proteins.

Western blotting

Protein immunodetection was performed as previously described (Neveu et al., 2016). Briefly, 20 µg of protein samples were diluted in Laemmli buffer and migrated on SDS-denaturating 10% polyacrylamide gels. Transfer was performed overnight at 4°C on polyvinylidene difluoride membranes. Membranes were then blocked in a milk solution prior to immunoblotting using the following antibodies anti-ETV6 (ab54705, Abcam, Cambridge, UK), anti- GAPDH (sc-31915, Santa Cruz Biotechnology, Dallas, TX, USA), Anti-β-Actin (sc-81178, Santa Cruz Biotechnology, Dallas, TX, USA), Anti-PCNA (ab92552, Abcam, Cambridge, UK). Immunodetection was performed by enhanced chemiluminescence with Western Lightning Plus-ECL (PerkinElmer, Waltham,MA, USA) according to the manufacturer's protocol.

Mass spectrometry

Pre-washed anti-HA magnetic beads (Thermo Fisher Scientific, Waltham, MA, USA) were added directly to nuclear and cytoplasm protein extracts from 5× 10^7 Reh pCCL ETV6 and ETV6-HA cells. After 4 hours of incubation with agitation at 4°C, beads were washed on a magnetic stand using 50mM ammonium bicarbonate. The on-beads digest and mass spectrometry experiments were performed by the Proteomics platform of the CHU de Quebec Research Center, Quebec, Canada.

Briefly, proteins on beads were washed 3 times with 50mM ammonium bicarbonate buffer and digested with Trypsin (1µg) 5 hours at 37°C then desalted on stage tip (C18) and vacuum dried before MS injection.

Peptide samples were separated by LC-MS/MS on an Ekspert NanoLC425 (Eksigent) coupled to a 5600+ mass spectrometer (AB Sciex, Framingham, MA,USA) equipped with a nanoelectrospray ion source. Peptides were separated with a linear gradient from 5-35% solvent B (acetonitrile, 0.1% formic acid) in 35 minutes, at 300 nL/min on a picofrit columns (Reprosil 3u, 120A C18, 15 cm × 0.075 mm internal diameter). Mass spectra were acquired using a data dependent acquisition mode using Analyst software version 1.7. Each full scan mass spectrum (400 to 1250 m/z) was followed by collision-induced dissociation of the twenty most intense ions. Dynamic exclusion was set for a period of 3 sec and a tolerance of 100 ppm

Database searching

MGF peak list files were created using Protein Pilot version 5.0 software (Sciex) then searched was performed using Mascot (Matrix Science, London, UK; version 2.5.1) on the CP_HomoSapiens_9606 database (92237 entries) assuming the digestion enzyme trypsin. Mascot was searched with a fragment ion mass tolerance of 0,100 Da and a parent ion tolerance of 0,100 Da. Deamidation of asparagine and glutamine and oxidation of methionine were specified in Mascot as variable modifications.

Criteria for protein identification

Scaffold (version Scaffold_5.0.1, Proteome Software Inc., Portland, OR) was used to validate MS/MS based peptide and protein identifications. Peptide and protein identifications were filtered with a FDR (false discovery rate) less than 1,0 % by the Scaffold Local FDR algorithm. Proteins that contained similar peptides and could not be differentiated based on MS/MS analysis alone were grouped to satisfy the principles of parsimony.

qRT-PCR

Total RNA was extracted from cells using the RNeasy Mini kit (Qiagen, Hilden, Germany) according to the manufacturer's protocol and quantified by Nanodrop (Thermo Fisher Scientific, Waltham,MA, USA). 750 ng of RNA were used for reverse transcription using the M-MLV reverse transcriptase (Life Technologies, Carlsbad, CA, USA). These cDNAs were then subjected to quantitative real-time PCR. Reactions were performed in triplicates using the SYBR Green PCR Master Mix (Life technologies, Carlsbad, CA, USA) and the primers listed in Table S5 on the ABI PRISM 7000 sequence detection system (Life Technologies, Carlsbad, CA, USA). Relative expression was calculated by the $2^{-(\Delta\Delta Ct)}$ comparative method (Livak and Schmittgen, 2001) using *GAPDH* and *β2M* as reference genes.

Transcriptome analysis of cancer patients

Transcriptome data from childhood ALL patients and controls were obtained from a previous study (Lajoie et al., 2017). Additional childhood B-ALL patients (11 t(12;21) positive and 14 t(12;21) negative) and controls (3 $CD19^{+}CD10^{+}$ pre-B cells isolated from healthy cord blood samples) were also included. Briefly, white cells from bone marrow samples were enriched with Ficoll-Paque PLUS (GE Healthcare Life Sciences, Piscataway, NJ, USA). DNA and RNA from these cells were then extracted using the Allprep DNA/RNA mini kit (Qiagen, Hilden, Germany). 1 μg of RNA with RIN ranging from 5 to 10 were treated with DNAse (Ambion, Austin, TX, USA). Libraries were generated using the Illumina TruSeq Stranded Total RNA rRNA removal GOLD kit according to the manufacturer protocol. Sequencing was performed on the HiSeq 2500 system (paired-end 100 b.p.; Illumina, San Diego, CA, USA) with 8×10^{7} expected reads per sample. The pipeline to produce the RNAseq binary alignment files (BAM) is based on the GATK Best Practice for germline SNPs and Indels in RNAseq. The gene expression values (FPKM) were calculated using the Cufflinks tool version 2.2.1 (Trapnell et al., 2010) on hard-clipped BAM files.

TCGA normalized expression values (rundate '20160128') were obtained using the R package RTCGAToolbox v.2.0.0 (Samur, 2014). For each cancer, a log fold change was calculated for each gene using their median expression in the top and bottom 10% of *ETV6* expressing samples. 20 genes with the most negative fold changes were retained for further analysis. Additionally, 20 random genes with log fold changes near 0 (over -0.001 and under 0.001) were used as control genes uncorrelated to *ETV6* expression. Log fold changes for those cancer-specific *ETV6*-correlated and non-correlated genes as well as for known *ETV6* target genes were calculated similarly with the top and bottom 10% of samples according to the expression of each modulator.

QUANTIFICATION AND STATISTICAL

Data management and statistical analysis were performed using Excel (Microsoft, Redmond, WA, USA) and GraphPad Prism 5 software (GraphPad Software, San Diego, CA, USA). Data are reported as mean ± standard deviation (SD). Wilcoxon and Student t-test and were used to statistically compare two groups (as noted in the figure legend) and significance was set to $p < 0.05$ (***$p < 0.001$, **$p < 0.01$, *$p < 0.05$).